

Making In Vitro Tumor Models Whole Again

Kenny Zhuoran Wu, Christabella Adine, Aleksandr Mitriashkin, Benjamin Jun Jie Aw, N. Gopalakrishna Iyer, and Eliza Li Shan Fong*

As a reductionist approach, patient-derived in vitro tumor models are inherently still too simplistic for personalized drug testing as they do not capture many characteristics of the tumor microenvironment (TME), such as tumor architecture and stromal heterogeneity. This is especially problematic for assessing stromal-targeting drugs such as immunotherapies in which the density and distribution of immune and other stromal cells determine drug efficacy. On the other end, in vivo models are typically costly, low-throughput, and time-consuming to establish. Ex vivo patient-derived tumor explant (PDE) cultures involve the culture of resected tumor fragments that potentially retain the intact TME of the original tumor. Although developed decades ago, PDE cultures have not been widely adopted likely because of their low-throughput and poor long-term viability. However, with growing recognition of the importance of patient-specific TME in mediating drug response, especially in the field of immune-oncology, there is an urgent need to resurrect these holistic cultures. In this Review, the key limitations of patient-derived tumor explant cultures are outlined and technologies that have been developed or could be employed to address these limitations are discussed. Engineered holistic tumor explant cultures may truly realize the concept of personalized medicine for cancer patients.

resulting in less than 50% of patients responding to these non-targeted drug regimens.^[2] Accordingly, the concept of 'precision cancer therapy' emerged. In this approach, patient-specific genetic abnormalities are identified using next-generation sequencing, and drugs targeting these abnormalities, if available, are administered to the patient. For instance, the overexpression of human epidermal growth factor 2 (HER2) in about 20% of breast cancer patients has led to development of trastuzumab-based anti-HER2 therapy,^[3] where a 20% increase in response rate relative to conventional therapies was observed.^[4] Improved clinical outcome has similarly been observed in the use of anti-epidermal growth factor receptor (EGFR),^[5] anti-BRAF,^[6] and anti-c-KIT^[7] therapies for lung, melanoma, and gastrointestinal stromal cancers, respectively. However, the interim assessment of several ongoing precision oncology trials (e.g., NCI-MATCH,^[3] NCI-IMPACT,^[8] ALCHEMIST,^[9] SHIVA,^[10] etc.) has revealed that many of these targeted

1. Introduction


Despite advances in the development of novel cancer-targeting approaches, effective drug combinations, accurate patient selection, and rational application of other therapeutic modalities, cancer is still a major burden of disease worldwide, accounting for nearly 17% of deaths in 2020.^[1] A key limitation of traditional chemotherapies is the 'one-size-fits-all' paradigm,

approaches resulted in surprisingly undesirable clinical outcomes, where there was generally lower-than-expected progression-free survival (< 4 months).

The lack of widespread success of genomics-based approaches in precision oncology has led to an increased appreciation for the importance of non-genetic mechanisms in driving cancer growth, progression, drug resistance, and survival.^[3b,11] The inherent spatiotemporally changing complexity of the tumor

K. Z. Wu, C. Adine, A. Mitriashkin, B. J. J. Aw, E. L. S. Fong
Department of Biomedical Engineering
College of Design and Engineering
National University of Singapore
Singapore 119276, Singapore
E-mail: bieflse@nus.edu.sg

N. G. Iyer
Department of Head and Neck Surgery, Division of Surgery and Surgical
Oncology
Duke-NUS Medical School
Singapore 169857, Singapore
N. G. Iyer
Department of Head and Neck Surgery
National Cancer Centre Singapore
Singapore 169610, Singapore
E. L. S. Fong
The N.1 Institute for Health
National University of Singapore
Singapore 117456, Singapore
E. L. S. Fong
Cancer Science Institute (CSI)
National University of Singapore
Singapore 117599, Singapore

 The ORCID identification number(s) for the author(s) of this article can be found under <https://doi.org/10.1002/adhm.202202279>

© 2023 The Authors. Advanced Healthcare Materials published by Wiley-VCH GmbH. This is an open access article under the terms of the Creative Commons Attribution-NonCommercial License, which permits use, distribution and reproduction in any medium, provided the original work is properly cited and is not used for commercial purposes.

DOI: 10.1002/adhm.202202279

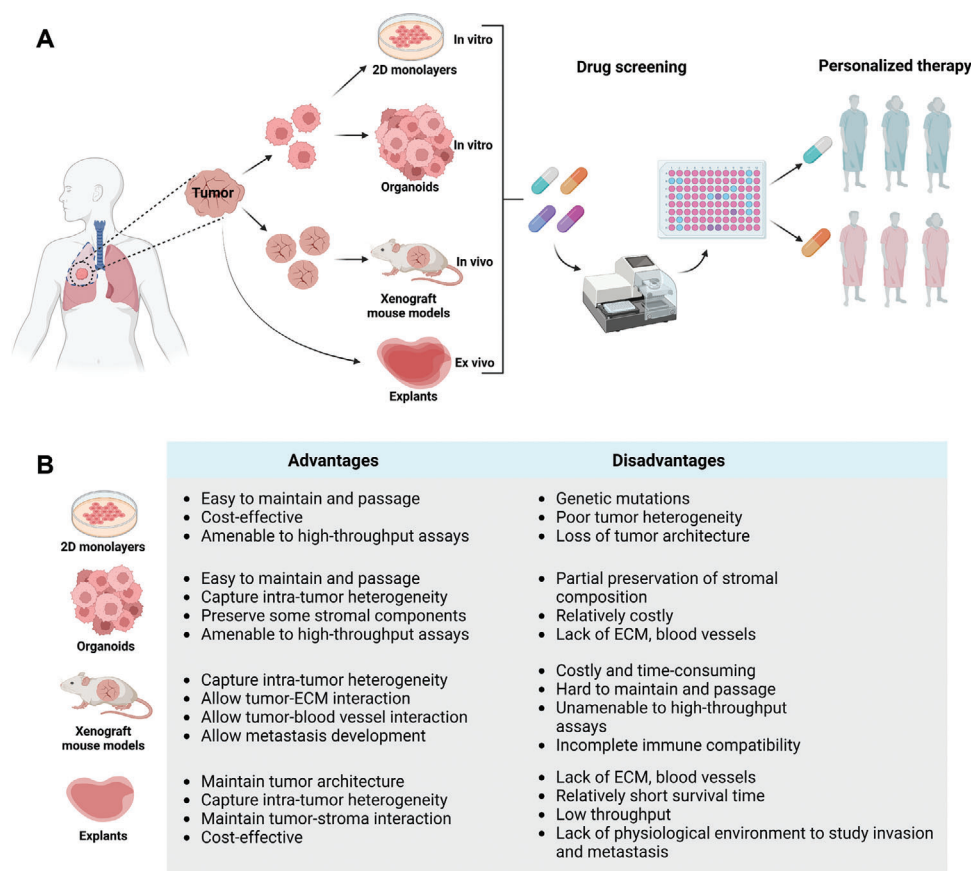


Figure 1. A) Existing tumor models used for preclinical drug testing and personalized therapy. B) Table summarizes the advantages and disadvantages of different preclinical tumor models. Created with BioRender.

microenvironment (TME) architecture and composition, is not taken into account in genomics-based (static) approaches.^[11,12] It is now clear that reciprocal interactions between cancer cells and their stromal counterparts, such as cancer-associated fibroblasts (CAFs),^[13] mesenchymal stem cells (MSCs),^[14] endothelial cells,^[15] and various immune cell types,^[16] can greatly influence tumor metabolism and chemosensitivity.^[17] This complex cancer-stromal ecosystem altering the tumor epigenetic state has been correlated to the highly discrepant susceptibility to drugs that is seen not only across different tumors but also in subpopulations within the same tumor.^[18] In addition, other TME factors such as inflammation,^[19] hypoxia,^[20] nutrient supply,^[20] and extracellular matrix (ECM)^[21] can also affect the cancer cell phenotype.

In contrast to static genomics-based approaches, functional precision oncology allows the actual testing of drugs on living cells and derivation of response readouts.^[3b] The use of in vitro tumor models as a preclinical model for functional precision oncology is not new; 2D monolayer cultures have been used for decades and remain widely used for testing drug efficacy and identifying novel cancer-targeting mechanisms (Figure 1).^[3b,22] However, 2D tumor models poorly preserve the tumor architecture, stromal composition, and when passaged repeatedly on tissue culture plastic, these cultures may also lose the original heterogeneity in cancer cell composition.^[23] In recent years,

the advent of patient-derived organoid (PDO) technologies has revolutionized in vitro tumor modeling, where patient-derived cancer cells can now be cultured and expanded with high success rates while maintaining molecular and histological features of the original tumor. Conventionally, PDOs are typically generated by dissociating resected tumors or biopsies into single cells, which would eventually form tumor organoids in the presence of a specialized cocktail of cell culture supplements and basement membrane matrix.^[24] As these are largely cancer cell-only cultures, the TME can be partially restored through the incorporation of desired stromal elements of interest.^[25] However, as a reductionist model, PDOs with exogenously incorporated stroma still poorly recapitulate the original complex tumor architecture and stromal heterogeneity.^[24,26] On the other end, in vivo patient-derived xenografts (PDXs) that involve transplantation and propagation of human tumor tissues into immunocompromised murine hosts, can preserve tumor heterogeneity and the surrounding stroma, except the interaction of cancer and stromal cells with a patient-specific immune system.^[11] Integration of either patient-derived immune cells or human immune transgenes into murine hosts can potentially overcome this problem,^[11] but these humanized PDXs are high in costs, the tumor takes a long time to engraft, the tumor may not engraft, and there still exists incomplete immune-compatibility.^[25,27]

In recent years, growing recognition that the assessment of stromal-targeting therapeutic approaches, such as immunotherapies, requires tumor models that retain the original architecture and stromal cell distribution and composition, has led to revived interest in patient-derived tumor explant (PDE) models.^[3b,28] PDE cultures are established when resected tumors are cut into smaller pieces and cultured *ex vivo*. The term 'PDE' is loosely defined and is often used interchangeably with patient-derived tumor slices (if cut into fragments with uniform thickness), and occasionally is referred to as organotypic cultures.^[28a] PDE cultures are advantageous over reductionist *in vitro* models such as those based on organoid cultures because: i) the tumor tissue is cultured as it is with minimal mechanical/enzymatic destruction of cell–cell and cell–ECM interactions, as is typically required for the generation of PDO models through extensive tumor dissociation; ii) PDE cultures potentially retain the full composition of original tumors, including the immune compartment; iii) PDE cultures are amenable for rapid drug testing (there is no need for an expansion step) and can provide readouts within a week from tumor resection or biopsy. Indeed, the histoculture drug response assay (HDRA) was developed shortly after the first successful human tumor histoculture was reported by Hoffman's group in 1986.^[11] Interestingly, despite exhibiting greater than 85% accuracy in predicting drug response in gastric, colon, and lung malignancies, histocultures have not been widely adopted for translational research.^[29] A likely reason for this may be related to some of the major limitations of tumor explant cultures, including its short lifespan *ex vivo* (generally < 7 days) and these cultures cannot be expanded. With these constraints, it is difficult to perform studies on treatment cycles, cancer progression, or drug resistance, that typically require a longer period of time (weeks to months).^[30]

To enable the culture of PDE, a number of different culture approaches including free-floating, air-liquid interface (ALI), and gelatin sponges have been employed and optimized over the last few decades. Overall, these studies broadly demonstrate that PDE can preserve tumor proliferation, histological features, and are amenable for the evaluation of chemotherapeutics.^[28b,31] However, the lifespan of these cultures is typically limited to a few days and characterization of PDE viability is poor.^[32] Specifically, it is unclear from these studies whether the stromal and immune compartments are preserved, in addition to the cancer cells residing in the explant. Besides poor long-term viability, other limitations of existing PDE models include their low throughput due to limited tissue availability, lack of sophisticated drug response readouts, and lack of integration with the systemic circulation and other tissues/organs that may impact drug response. In this Review, we provide an overview of conventional approaches that have been developed to establish PDE cultures, outline key limiting factors that hinder clinical translation of the model, and discuss possible engineering strategies and technologies that can be used to overcome some of these challenges.

2. Conventional Approaches for Maintaining PDE Cultures

Historically, PDE cultures have been maintained either free-floating without any underlying support, or cultured on top of metal grids, gelatin sponges, or hydrophilic polytetrafluoroethy-

lene (PTFE) cell culture inserts, to establish an ALI to overcome diffusional limitations (**Figure 2A**). In this section, we describe these conventional methods.

2.1. Gelatin Sponge-Based Cultures

The first tumor PDE studies were pioneered by Leighton et al. Murine mammary adenocarcinoma fragments were maintained on a collagen-coated cellulose sponge for up to 24 h.^[33] Subsequently, Freeman et al. were the first to report successful *ex vivo* culture of surgically resected human tumor fragments on collagen hydrogels.^[31a] Extended culture (> 100 days) of a broad range of cancer types including colon, lung, and melanoma was achieved. It should be noted that cells that escaped from the tissue and migrated into the hydrogel, and subsequently grew on the culture dish as monolayers, were also taken into consideration as part of viability assessment of the tumor fragments. This may have contributed to an over-estimation of the duration these tumor tissues could actually be maintained *ex vivo*.^[31a] Besides collagen hydrogels, gelatin sponges have also been used for PDE culture. Gelatin sponges have proved useful for the culture of PDE derived from breast,^[34] prostate,^[35] head and neck,^[36] and pancreatic ductal adenocarcinoma (PDAC) cancers (**Figure 2B,C**).^[31b] Further applications of this model for preclinical drug testing,^[37] biomarker discovery,^[38] and interrogation of tumor interactions with the surrounding microenvironment^[39] have also been reported.

Yet, it is often observed that PDE exhibits rapid loss in tissue integrity and viability (often < 6 days) when cultured on gelatin sponges.^[34,40] This is likely in part due to manual cutting of samples into fragments, which confers poor control over the resulting size and shape of the tumor fragments. This problem has been resolved through the development of newer tissue slicing technologies, such as tissue choppers, vibratomes (Vibratome), and compressotomes.^[41] With these improved methods for tissue processing, tumor samples can be precisely cut into slices with a uniform thickness range of 30–1000 μm .

2.2. Free-Floating Cultures

With precision-cut tissue slices, the simplest method to culture these slices is to completely submerge them in cell culture medium without any underlying support.^[31c] Not surprisingly, the integrity of these slices can only be maintained for a short duration (< 48 h) due to inadequate oxygen supply. Since then, rocking or rotating platforms^[42] have been used to extend the lifespan of tissue slices by facilitating gas diffusion. Naipal et al. reported that maintenance of proliferative cells in human breast tumor slices was highly dependent on the use of rotational dynamic culture to increase nutrient exchange.^[43] Another study by Davies et al. found that tumor slices from breast and lung cancer were better maintained within a rotary incubation unit as compared to free-floating, as significantly less cell necrosis and lower stress marker expression were observed.^[44]

2.3. ALI Cultures

In seeking to improve the diffusion of oxygen into tumor tissue slices, many groups have leveraged the use of metal (such as

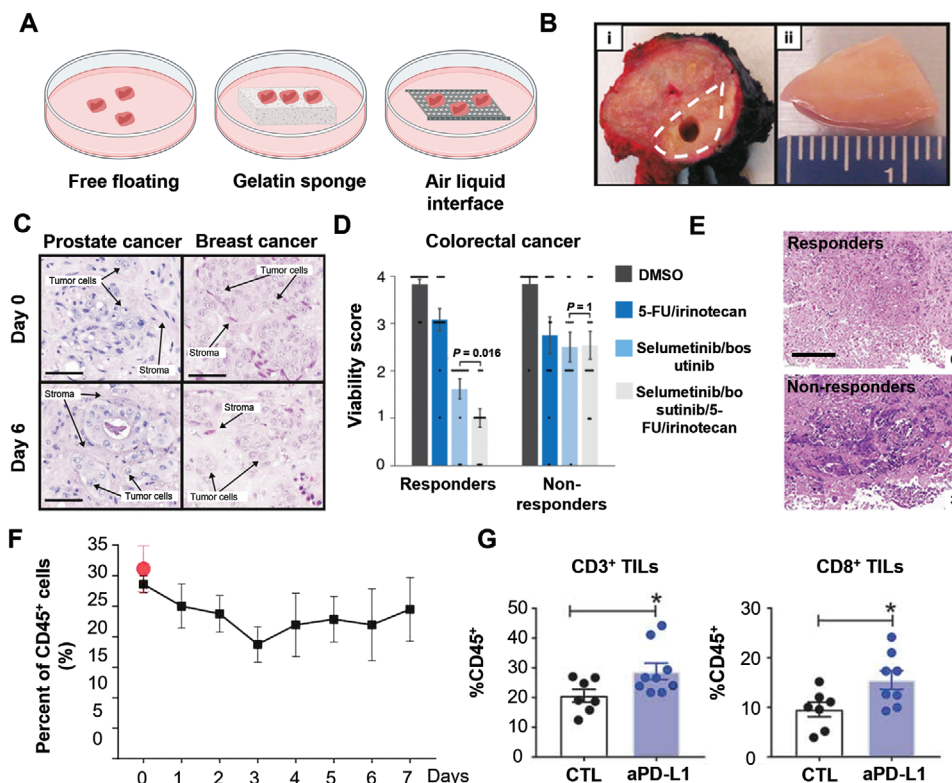


Figure 2. A) Schematic of conventional PDE culture methods. Created with BioRender. B) Representative images that describe tumor tissue processing after resection. i) Following surgery, a core of tumor tissue is removed by a pathologist (tumor area demarcated by broken white line), ii) the tumor sample is then dissected into 1 mm³ fragments.^[31] Reproduced with permission.^[31b] Copyright 2021, FEBS Press. C) Representative hematoxylin and eosin (H&E) staining of PDEs from primary prostate and breast tumors, showing maintenance of gross morphology following 6 days in gelatin sponge-supported culture. Arrows indicate examples of cancer cells and surrounding stroma.^[31] Reproduced with permission.^[31] Copyright 2021, FEBS Press. D) Bar graph summarizing the average viability of patient-derived colorectal cancer (CRC) slices (n = 26) in response to treatment with 5-FU and irinotecan, selumetinib, and bosutinib or the combination of all four drugs. CRC slices were cultured on organotypic culture inserts and drug combinations were added on days 1, 4, and 7. Viability of the tumor slices was assessed daily and viability score was obtained by normalizing the viability of slices at each time point to that on day 0.^[28] E) Representative histological sections of CRC tumor slices, which were stained with H&E, and correspond to the data shown in (D). Scale bar = 100 μm.^[28] Reproduced with permission.^[28b] Copyright 2022, Springer Nature. F) Plot shows percentage of CD45⁺ leukocytes in pancreatic tumor slices over a period of 7 days in culture.^[46] G) Bar charts showing % of CD3⁺ (left) and CD8⁺ (right) tumor-infiltrating lymphocytes (TILs) in liver tumor slices after anti-PD-L1 treatment. Increase in CD3⁺ and CD8⁺ T cells indicates enhanced anti-tumoral effect. * denotes p < 0.05.^[46] Reproduced with permission.^[46] Copyright 2019, Taylor & Francis Group.³¹

titanium) grids^[45] or porous membrane cell culture inserts^[28b,44] to create an ALI. Compared to free-floating cultures, the viability of MCF-7 derived PDX slices was better maintained (within 48 h) when the slices were cultured on organotypic culture inserts with atmospheric oxygen.^[44] Using a similar approach, Gavert et al. leveraged tumor slice cultures for testing drug combinations in colorectal cancer (CRC) and showed that these cultures could identify patient subgroups responsive to the drug combinations, highlighting the possibility of using tumor slice cultures for determining patient response to chemotherapeutic drugs (Figure 2D,E).^[28b] Amongst different ALI cultures, PTFE cell culture inserts are most commonly employed due to its simple set-up and ease of use.^[45] PTFE has a pore size of 0.4 μm, exhibits mesh-like topography, and has a fibrous structure with high permeability and porosity which allows transport of nutrients across the whole (bottom) surface of tissue slices placed on top. PTFE membranes have been used to establish PDE models across a broad range of cancer types. For example, Sivakumar

et al. showed that tumor slices from liver cancer retained various immune subpopulations and were responsive to immune modulators after 7 days in PTFE-based culture, highlighting the potential of using tumor slices for studying tumor-immune interactions and evaluation of immunotherapies (Figure 2F,G).^[46] Parker et al. demonstrated live tracking of cancer cells using viral vectors on PTFE-cultured tumor slices for real time assessment of cell behavior within an intact TME.^[47] To adhere tissue slices onto the underlying PTFE membrane surface, tumor slices have been cultured on laminin-^[48] or collagen-^[48] coated PTFE and improved slice preservation was observed. However, while PTFE membranes are easy to use and enable the maintenance of tumor slices for a few days in culture, this platform is still not optimized in terms of biochemical and/or mechanical properties as a tissue-supporting substrate. In the next section, we will discuss how PTFE can potentially be replaced by bioengineered scaffolds with tunable biophysical and/or biochemical cues, as one of the strategies for enhanced preservation of PDE ex vivo.

3. Strategies to Overcome Limitations of PDE Models

While significant bioengineering advances (biomaterials-based scaffolds, bioreactors, microfluidic systems, etc.) have been made to maintain and grow single cells and spheroids in vitro in the field of tissue engineering, surprisingly little has been done to improve the culture of tissue or tumor explants. In this section, we outline key factors that limit PDE models — poor long-term viability, low throughput, lack of sophisticated readouts for characterization and drug response, and lack of integration with other tissue/organ systems — and propose technologies that have been or can be explored to overcome these challenges.

3.1. Limited PDE Viability

One of the key factors that limit the use of PDE models is poor long-term viability *ex vivo*. There may be several potential contributing factors to this problem, which we have identified and will discuss in the following sections — hypoxia, failure to maintain the immune compartment, lack of tumor-matched matrix for PDE culture, and poorly optimized PDE culture medium composition.

3.1.1. Overcoming Hypoxia within PDE

The vascular system plays a critical role in ensuring large tissues and organs receive sufficient oxygen and nutrients while permitting waste exchange.^[49] Hypoxia arises when there is insufficient oxygen delivered to tissues, a phenomenon that often leads to necrosis within tumors in vivo. Following tumor excision, as the resected tissues are cut off from the systematic circulation, this can lead to hypoxic conditions within the PDE. Given that cells at a distance of > 150 μm from blood vessels in vivo likely experience hypoxia,^[49] and PDE is typically greater than 200 μm in dimension, it is expected that hypoxia may occur within the tissue. Indeed, Lee and colleagues reported the presence of hypoxic cores in head and neck squamous cell carcinoma (HNSCC) PDE cultures (Figure 3A,B).^[50] Similar findings were reported by Dorrigiv et al. for ovarian and prostate cancers.^[51] As the level of hypoxia depends on location within the PDE fragment, this *ex vivo* artifact may contribute to intra-tumoral differences in cell proliferation and density, an undesired outcome of PDE culture.

How can hypoxia be circumvented in PDE cultures? The most straightforward strategy to overcome hypoxia is to reduce PDE thickness, given its inverse relationship to oxygen diffusivity across the tissue. However, to generate PDE of thickness below 150 μm would render sample handling extremely difficult.^[45,52] Although there is no optimal tissue thickness, most groups report a range of 200–300 μm for slice thickness. To further increase diffusion of oxygen into PDE, several groups have proposed dynamic culture systems where biophysical forces are incorporated into the culture system to enhance gas and nutrient transport. The simplest way to achieve this is by orbital shaking. This dynamic approach follows the same protocol as the static ones, except that samples are cultured on an orbital shaker. Hoogt et al. conducted a systematic comparison of their in-house rotating culture system with conventional free-floating and insert-based ALI

cultures to evaluate the effect of dynamic culture on non-small cell lung carcinoma (NSCLC) PDE viability. The authors showed that the rotating culture system contributed to long-term tissue viability and integrity *ex vivo*.^[53] A similar agitation-based approach developed by Abreu et al. allowed ovarian cancer PDE to remain viable and preserved cell type integrity and histological architecture for up to 30 days, a significant improvement over the commonly reported 2–7 days (Figure 3C,D).^[54] While relatively simple to execute, orbital shakers provide poor control over shear stress, which may make mechanistic studies on the effect of shear stress on hypoxia and cell survival challenging.^[55] Moreover, there is no active perfusion through the tissue.

In contrast, perfusion bioreactors equipped with a flow-through chamber and dynamic pump system permit a high degree of control over fluid flow rate. In a report by Manfredonia et al., compared to colorectal PDE embedded between two collagen type I discs, tissues embedded in collagen discs and connected to a perfusion device retained > 75% (versus 31% in the static control) of the original PDE weight 3 days post-culture (Figure 3E).^[56] Using a similar setup, Huo et al. demonstrated successful maintenance of neuroblastoma PDE *ex vivo* for up to 10 days.^[57] Recently, advances in microfluidic technologies have enabled the integration of perfusion bioreactors and microfluidics; these micro-bioreactors are advantageous over traditional bulky bioreactors due to its microscale geometry, which allows for a more physiologically relevant environment for gas and waste exchange.^[58] The first tumor PDE in a micro-bioreactor was pioneered by Folch's group (Figure 3F).^[59] In their approach, perfusion-based microfluidic channels were designed to integrate with 96-microwell plates to allow for high throughput and multiplexed screening of a large number of drugs (up to 80) on a single glioblastoma (GBM) slice (Figure 3F). By comparing calcein-AM staining of the samples cultured on PTFE to that on polyethylene terephthalate (PET)/ polycarbonate (PC) porous membranes, the authors found that PTFE outperformed PET and PC in maintaining viability of the tumor slices in a 3-day period. However, although the applied drugs (i.e., staurosporine, temozolomide) were designed to affect a distinct section of the tumor slice, it is unclear whether the drugs generate off-target effects on areas near the designated working area in the tissue, thereby possibly leading to skewed data interpretation. Interestingly, by refining the diameter of tumor slices to micrometer scale (about 400 μm) and exploiting the gas-permeable property of polydimethylsiloxane (PDMS), Astolfi et al. noted that perfusion is not actually necessary for PDMS-based microfluidic devices to retain the viability of tumor slices in an 8-day culture period.^[60] Using a simple microfluidic setup, the authors devised a histoculture strategy that can enable rapid drug testing on an one-drug-per-slice format (Figure 3G).

Rather than using perfusion to increase the diffusion of oxygen into PDE, it is also possible to overcome hypoxia by incorporating oxygen-releasing molecules into the culture system. Oxygen sources that have been investigated include metal peroxides (e.g., calcium peroxide, magnesium peroxide), liquid peroxides (e.g., hydrogen peroxide), and fluorinated compounds (e.g., perfluorocarbon). Direct addition of these oxygenated agents often results in burst release of oxygen into the culture medium, which is cytotoxic. This problem has been resolved through the use of advanced drug delivery technologies, which encapsulate oxygen

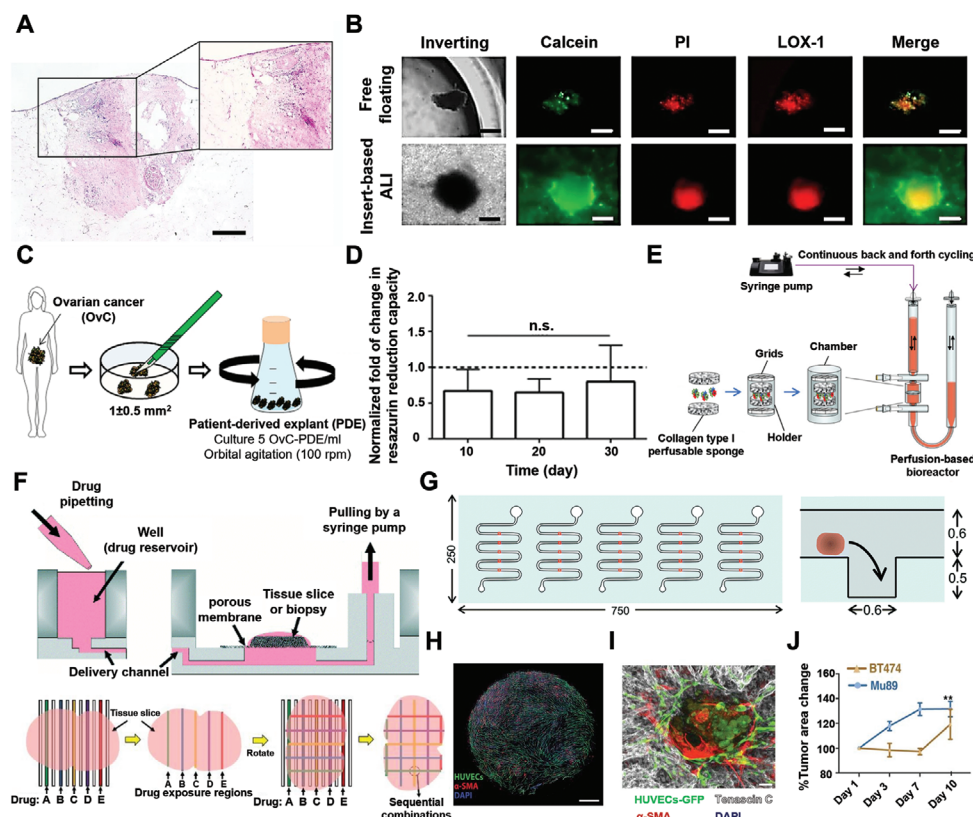


Figure 3. A) H&E staining of tumor explants in an insert-based 3D culture. Necrotic zone is clearly seen in the zoom-in inset image. Scale bar = 100 μ m. B) Representative images show the hypoxic cells identified with LOX-1 staining (red) after 5 days of being cultured free-floating or with cell culture inserts. The non-viable area was stained with PI (red) and the live tissue areas were stained with calcein-AM (green). Scale bar = 100 μ m. Reproduced with permission.^[50] Copyright 2020, Springer Nature. C) Schematic representation of the agitation culturing strategy employed for ovarian cancer (OvC) PDE culture. D) Resazurin reduction capacity of the OvC-PDE on days 10, 20, and 30 relative to day 0. Data are presented as mean \pm SD ($n \geq 7$). Reproduced with permission.^[54] Copyright 2020, Springer Nature. E) Schematic representation of perfusion-based PDE culture. Freshly resected CRC fragments ($2 \times 2 \times 2$ mm) were placed between two collagen type I discs within a ring-shaped holder, restrained by two grids on the top and bottom. The holder was then inserted in the bioreactor chamber and subjected to continuous alternate perfusion. $n = 3$ per bioreactor. Reproduced with permission.^[56] Copyright 2019, Wiley-VCH GmbH. F) Schematic of cross-sectional view of the device (left) and action principle of sequential drug delivery to tumor tissue slices (right). The flow of the device is driven by a syringe pump through a common outlet: one syringe pump controls the flow across all 80 fluidic streams. After delivering the first set of drugs, the porous membrane can be rotated 90 degrees to deliver a second set of drugs. Reproduced with permission.^[59] Copyright 2014, Royal Society of Chemistry. G) Top view (left) and side view (right) of a microfluidic device. Tumor explants are designed to flow into and get trapped by sedimentation trap for drug testing. Dimensions in mm. Reproduced with permission.^[60] Copyright 2016, Royal Society of Chemistry. H) A fluorescence micrograph shows the complete vascular network across the entire well of a 96-well plate. Scale bar = 800 μ m. I) Interaction of Mu89 (melanoma) explants with vascular networks. Mu89 expressed strong level of tenascin-C (grey). Scale bar = 100 μ m. J) Growth curves for Mu89 and BT474 (breast cancer) in 10-day culture. Reproduced with permission.^[64b] Copyright 2016, Oxford Academic.^[50,54,56,59,60,64]

sources into either organic (e.g., alginate)^[61] or inorganic (e.g., Bi_2Se_3)^[62] biomaterials that enable sustained or on-demand gas release. To date, a wide range of oxygen-releasing biomaterials have been developed and applied in bone regeneration, cardiac ischemic therapy, tumor treatment, and wound healing.^[63] To the best of our knowledge, oxygen-releasing biomaterials have not been used for PDE culture to date. Engineering an advanced material that can control the release of oxygen and is compatible with PDE cultures may potentially overcome this problem of hypoxia in PDE cultures.

Lastly, given the importance of the vasculature for providing oxygen to tumors in vivo, another possible solution to overcome hypoxia in PDE cultures is to induce vascularization ex vivo. De novo synthesis of functional blood vessels can be achieved by co-

culturing vascular endothelial cells and smooth muscle cells in a matrix comprising ECM components and growth factors.^[64] Such artificial vascular beds were first used for tissue regeneration and wound healing but recent studies have also demonstrated the use of these set-ups for maintaining PDE cultures. PDE can be placed on top of vascular beds to recapitulate interactions between tumor and blood vessels. As an example, melanoma and breast cancer PDEs cultured on a scaffold containing lumenized vascular structures were shown to survive and proliferate ex vivo for up to 10 days (Figure 3H–J).^[64b] To mimic the 3D interaction of tumors with the in vivo vasculature, vascular constructs can be fabricated in a complex integrated system based on either microfluidic or 3D printing technologies. This will be discussed in greater detail in Section 3.4.

3.1.2. Preservation of Immune Landscape in PDE

Poor consideration for what constitutes preservation of PDE viability is another contributing factor to the limited long-term viability of PDE cultures. The maintenance of PDE viability does not only include preserving global viability of the explant. Many different cell types and subtypes make up the TME, including cells within the immune compartment. Preserving cells within the immune compartment is especially important were PDE cultures used for evaluating immunotherapies. A recent study by the Thommen group highlighted the problem of immune cell efflux from PDE cultures, which justified the need to embed the tumor fragments within a 3D matrix.^[65] However, most studies to date do not deeply characterize whether PDE preserves immune cell types and subtypes, such as T/B cells, mast cells, monocytes/macrophages, NK cells, neutrophils, amongst others.^[19] In a handful of studies, in-depth profiling of the immune landscape in PDE has been performed. By using gelatin sponges to support ex vivo slice culture of primary HNSCC, Dohmen et al. observed that T cells and macrophages were preserved during 7 days of culture, although significant changes in the proportion of subpopulations occurred.^[36] In another study, Jiang et al. established a PDE culture system that allowed slices derived from PDAC to freely float on collagen-coated inserts; this approach yielded stable preservation of T cell- and macrophage-specific markers over 6 days.^[66] In a recent study, Voabil et al. took a step further, where PDEs were shown to not only preserve the composition of immune cells, but also retained cell function (secretion of chemokines and cytokines) at the end of a 2-day culture period.^[28a] Notably, this PDE model, where tumor fragments were embedded in collagen-Matrigel, was reported to be compatible with a number of cancer types including skin, lung, breast, ovarian, and renal cancers, and was shown to be predictive of immune checkpoint inhibitor (ICI) response in patients. This landmark study has set the stage for PDE as a platform to test ICIs; however, it remains to be seen whether longer term drug exposure is required for the evaluation of ICI therapy or other drug classes, which would require culture of these PDE beyond just 48 h. Besides this handful of studies that have characterized whether PDE preserves the immune compartment, future studies reporting the development or use of PDE cultures should incorporate advanced characterization, such as multiplex immunofluorescence (mIF), multiplex immunohistochemistry (mIHC), flow cytometry, genomic and proteomic profiling into their experimental workflow, to determine how long these PDE cultures can preserve the immune TME.

To preserve PDE cultures longer in vitro for the evaluation of immunotherapies, microfabrication techniques have recently been leveraged to achieve this. For example, Aref et al. reported an extended culture (up to 9 days) of patient-derived organotypic tumor spheroids (PDOTS) for probing programmed cell death protein 1 (PD-1) blockade sensitivity, using microfluidic chips made of cyclic olefin polymer (COP).^[67] COP was used instead of commonly used PDMS as absorption of drug molecules onto PDMS may potentially occur, which can affect drug response.^[68] In another study, Moore et al. designed a COP-based microfluidic chip that allowed culture of up to 12 tumor explants per chip and real-time tracking of TILs interaction with the tumor explants in the presence of ICI treatment.^[68] These

advances in microfluidic systems are expected to greatly support both the preservation as well as recapitulation of the immune landscape in PDE cultures.^[69] In addition to preserving or recapitulating the original tumor immune landscape, it remains unclear whether PDE models permit interrogation of tumor response to systemic immunity, given the growing research interest in chimeric antigen receptor (CAR) T-cell therapy. As the vasculature is a prerequisite for such studies, using advanced microfluidics technologies to restore tumor–blood vessel interactions may be a promising means to recapitulate the tumor-immune interface. This topic will be further discussed in Section 3.4.

On another note, it should be highlighted that changes to the status of tissue inflammation may occur during tumor processing ex vivo. A handful of studies have already characterized the effect of chopping or slicing tissues (as part of tissue processing prior to ex vivo culture). These studies collectively demonstrate that chopping or slicing activates several inflammation-associated pathways,^[46,70] artificially inducing acute inflammation in PDE cultures. Yet, this source of inflammation and its possible effect on PDE viability has been largely disregarded in PDE research. Given the known role of acute inflammation in cancer cell proliferation and progression, it is reasonable to assume that existing PDE models may not truly recapitulate the baseline immune landscape of the original tumor. It would be of interest to explore mechanical manipulation of resected/biopsied tumors in a minimally destructive manner to reduce this inflammation-related artifact.^[71] It would also be interesting to explore whether certain anti-inflammatory drugs or biomaterials (e.g., hyaluronic acid, chitosan, fibrin)^[72] can be used to mitigate the artificial inflammatory response post-tissue processing.

3.1.3. Lack of Optimized PDE-Supporting Matrix

Another potential contributing factor to poor long-term PDE viability is the lack of optimized matrix support for PDE culture. A burgeoning number of studies in biomaterials highlight how cell phenotypes can be manipulated by modifying biochemical or physical properties of the culture matrix.^[73] Yet, carefully designed biomaterials-based scaffolds are rarely used to support PDE cultures, as PTFE insert-based ALI and free-floating (scaffold-less) cultures are conventionally used. While gelatin sponges have been used to support PDE cultures, there has been no significant increase in survival time compared to insert-based cell culture systems.^[31b,35,74]

While the effect of matrix support on PDE ex vivo cultures remains poorly elucidated, a few studies have compared the effect of different supports on tissue viability and proliferation. For instance, when cultured on a PTFE membrane cell culture insert, prostate tumor slices were found to be more viable compared to those suspended freely, as observed by the presence of fewer condensed apoptotic nuclei and vacuolated structures.^[44] This study highlighted the importance of providing an underlying support to PDE cultures. In another study, it was found that PTFE membranes outperformed PET and PC for retaining the viability of brain slices over a period of 3 days (Figure 4A).^[59] Another study reported successful retention of major immune (T cells, macrophages) and stromal components (CAF,

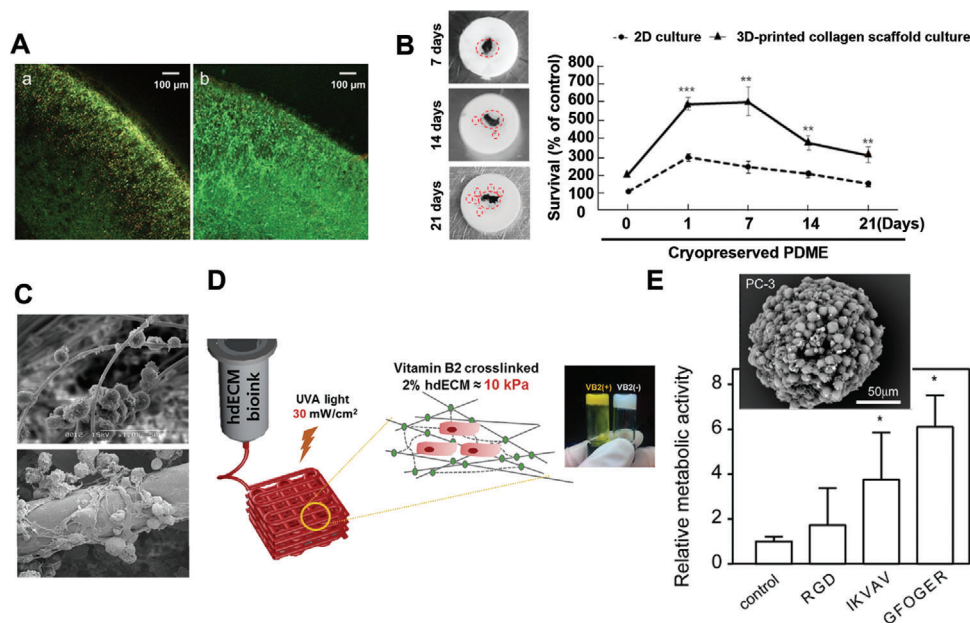


Figure 4. A) Representative confocal microscopic images show the viability of E18 mouse brain slices cultured on a) PET porous membrane and b) PTFE porous membrane under the same culture conditions. Live cells were stained with calcein-AM (green) and dead cells were stained with EthD-1 (red). Reproduced with permission.^[59] Copyright 2014, Royal Society of Chemistry. B) Representative images of 3D-printed collagen scaffolds loaded with cryopreserved patient-derived melanoma explants (PDME) at 7, 14, and 21 days. The graphs indicate proliferation of the 2D-culture and 3D-printed collagen scaffold culture at the indicated time points. Red circles show cryopreserved PDME and its satellite. Values represent the mean \pm SD of triplicate experiments. Significant difference from 2D-culture is indicated as ** ($p < 0.01$) and *** ($p < 0.001$). Reproduced with permission.^[75] Copyright 2021, MDPI. C) Representative SEM images of non-woven fabrics prepared from the PET fiber with diameters of 2.0 μm (top), 42.0 μm (down). PET with larger diameter and pore size between fibers is conducive for cell proliferation and spreading. Reproduced with permission.^[78] Copyright 2004, Taylor & Francis Group. D) Schematic illustration of the vitamin B2-crosslinked human derived ECM matrix (hdECM). The inset image shows the difference in physical appearance between non-crosslinked and crosslinked matrix. Reproduced with permission.^[90] Copyright 2016, Elsevier. E) Metabolic activity of PC-3 tumor organoids normalized to that at day 0 in the hydrogel after 7 days of culture. Significant differences ($p < 0.05$) compared to control are indicated (*). Inset image shows the SEM image of the PC-3 tumor organoid released from the hydrogel after 14-day culture. Reproduced with permission.^[102] Copyright 2016, Elsevier.^[59,75,78,90,102]

myofibroblasts) in PDAC slices after 6 days, by using collagen-coated PTFE membranes.^[66] This could be due to the mechanical anchorage of the slice through the collagen layer, or through recapitulation of tissue–ECM interactions. This finding was corroborated by Jeong et al., where there was a significant improvement in viability of patient-derived melanoma explants when these explants were cultured on a 3D-printed collagen matrix as compared to the control without collagen (Figure 4B).^[75] Adding other ECM components, such as fibronectin and laminin-derived short peptides into the matrix, was also found to be beneficial for maintaining precision-cut lung slices, where viability of the slices was extended from 7 to 21 days.^[76]

Given the importance of the ECM in mediating cell survival, PDE cultures may benefit from the use of optimized scaffolds with cancer-specific biochemical and/or biophysical properties to support the tissues ex vivo. However, this has not been investigated. In the following subsections, we briefly summarize recent findings on how biophysical properties of the ECM, such as the porous architecture, matrix stiffness, and cell adhesivity, can influence cell and organoid survival and phenotype. These examples may then serve as a starting point for optimizing matrices for PDE culture.

Optimizing Porous Geometry of Matrix: Scaffold porosity can play an important role in mediating cell viability and proliferation.

As larger pore size and higher porosity enable greater fluid diffusivity, nutrient and gas exchange, as well as waste removal, can be improved.^[77] When mesenchymal stem cells (MSCs) were cultured on a PET fibrous scaffold, it was observed that proliferation rate increased with fiber diameter and pore size (Figure 4C).^[78] Likewise, another study reported enhanced proliferation when human foreskin fibroblasts were cultured on 3D silk fibroin scaffolds with larger pore size and higher porosity.^[79] From these studies, it appears that the optimum porosity and pore size is likely material- and cell type- dependent, as the range of reported optimal pore size (8–700 μm) is very large.^[80] A systemic examination of pore size and porosity is thus necessary to determine the optimal scaffold porosity to support PDE culture. It should be noted that increased scaffold or hydrogel porosity is typically accompanied by a reduction in structural stability in accordance to the power-law relationship.^[81] Therefore, a fine balance between porosity and mechanical strength is necessary. Conventional techniques, such as salt leaching, gas forming, phase separation, and freeze-drying are commonly used to produce porous scaffolds.^[82] While these techniques are simple to set-up, they generally suffer from poor control over the scaffold architecture and thus lack batch-to-batch consistency.^[82] Rapid prototyping fabrication techniques (e.g., 3D printing) offer improved control over scaffold geometry and mechanical

properties with high reproducibility.^[82,83] For more information regarding the fabrication and application of porous/porosity gradient scaffolds, the reader is recommended to refer to other excellent reviews.^[84]

In the context of PDE culture, which has unique requirements distinct from the culture of cells, porosity may have to be tuned to enable optimized diffusion of nutrients, waste, and oxygen, while maintaining sufficient mechanical support. Additionally, it would be important to consider the pore size; large pore sizes may encourage migration of cells out of the PDE to form tumor aggregates within the pores, as has been observed for PDE cultures on collagen hydrogels.^[31a] In a similar vein, it may be important to consider the type of biomaterial used to fabricate the porous scaffold to limit the migration of cells out of the PDE itself (such as through controlling cell adhesivity). This may cause 'evacuation' of the explant and corresponding loss of tissue architecture and composition.

Optimizing Matrix Stiffness: It is well-known that cells respond to ECM stiffness, in vitro or in vivo. Modulation of matrix stiffness can influence cell differentiation, proliferation, and stemness.^[85] Numerous studies have leveraged advances in biomaterials engineering to fabricate scaffolds and hydrogels with varying stiffnesses to elucidate the effect of this mechanical property on the cellular phenotype.^[86] Yet, this strategy has not been employed in PDE culture, where PDE, regardless of tissue origin, is grown on the same matrix such as PTFE membrane inserts. Here, we will highlight a few studies which have shown how matrix stiffness can modulate cell/organoid growth. By extrapolating these findings from cells and organoids to PDE cultures, it would be interesting to investigate if cancer-type matched stiffness in material properties would similarly enhance the viability of PDE cultures.

Basement membrane extracts (BME) are widely used in tumor organoid cultures and would be a logical choice of biomaterial to start with for PDE culture. Indeed, as a commercially available BME, Matrigel was used to culture PDE from different cancer types, and when combined with collagen, mitigated immune cell loss from PDE cultures.^[28a] However, the PDE cultures were maintained for only 2 days. While used in many research groups, Matrigel itself may incite a non-specific immune response, exhibits batch-to-batch variation, and has poor tunability in mechanical properties.^[87] Another potential source of biologically-derived biomaterial is decellularized ECM (dECM), which has been investigated for maintaining organoids. In a study by Varinelli et al., peritoneal cavity-derived dECM was used for in vitro culture of tumoroids of peritoneal metastases.^[88] In this study, it was found that tumoroid growth was favored on the stiffer matrix obtained from the neoplastic peritoneum over that from the normal peritoneum, suggesting the importance of using tumor-matched matrix stiffness for PDE culture. While in vivo-like, the process of decellularization leads to changes in the native stiffness of the ECM due to collagen denaturation.^[89] One approach to overcome this is to tune dECM stiffness by altering the dECM concentration used for hydrogel fabrication. However, this can modulate stiffness only to a limited extent as increase in material concentration concomitantly leads to higher viscosity and difficulty in forming usable hydrogels.^[89] Another approach to modify dECM stiffness is by crosslinking. Jang et al. improved dECM stiffness by using vitamin B2 as a crosslinker (Fig-

ure 4D).^[90] Beyond basement membrane extracts and dECM, collagen, and hyaluronan (HA)-based biomaterials and their derivatives are also commonly used to explore the effect of stiffness on cells in vitro and may be useful for PDE culture.^[91]

Besides native ECM-derived biomaterials, synthetic polymers have also exhibited broad applications in in vitro tumor culture due to their defined chemical structure, reproducibility, and tunable mechanical properties.^[92] Although synthetic biomaterials are typically not cytotoxic, their lack of bioactivity hampers cell recognition and survival.^[92] Hybridization of synthetic polymers with natural biomaterials is thus often employed to further improve their biocompatibility.^[92] For example, gelatin and polyethylene glycol (PEG) can be mixed to form cell-supporting matrix with tunable mechanical properties.^[93] Jiang et al. and Pedron et al. exploited hybrid materials, building on the advantages of the inherent bioactivity of gelatin methacryloyl (GelMA) and tunable elasticity of PEG, for establishing osteosarcoma and glioblastoma models, respectively.^[94] As synthetic polymers generally lack integrin-binding domains, short peptides such as RGD that are derived from ECM proteins, can be incorporated into the hydrogel formulation to provide biochemical cues.^[76] To tune the stiffness of synthetic polymers, it can be achieved by crosslinking with either natural biomaterials like gelatin, or with chemical crosslinkers. The stiffness of PEG hydrogels can be controlled by light,^[95] or click reaction between norbornene and thiol ends of the polymeric chain,^[96] or by the concentration of matrix metalloproteinase (MMP)-sensitive peptides.^[97]

In sum, given the known influence of matrix stiffness on cancer cells,^[86d,89] the effect of this parameter on PDE viability and preservation urgently needs to be investigated.

Optimizing Matrix Adhesivity: Integrin-mediated cell adhesion is crucial for cells to sense and respond to mechanical stimuli in the surrounding matrix. Particularly after tumor resection and tissue processing, cells in the explant may experience anoikis in the absence of an underlying support. In designing a suitable matrix for PDE culture, matrix adhesivity may be an important parameter to adhere and mechanically anchor the explant. In fact, collagen has been used to 'glue' down tumor slices onto PTFE membrane inserts.^[66,98] Rather than using whole ECM proteins, an alternative may be to leverage ECM-derived peptides to systematically investigate the effect of different ECM components on maintaining PDE viability and composition. For example, non-adhesive synthetic polymers can be modified with fibronectin-derived peptides to enable integrin-mediated cell adhesion; RGD-modified PEG hydrogels have been shown to support growth of breast cancer,^[99] melanoma,^[100] and glioblastoma.^[101] Aside from RGD, peptides derived from laminin, such as IKVAV and YIGSR, and from collagen, such as GFOGER, have been used to facilitate cell adhesion onto non-adhesive matrices. In the case of aggressive prostate cancer, the presence of GFOGER in PEG hydrogels led to the highest growth rate of cultured cancer cells compared to RGD- and IKVAV- modified hydrogels (Figure 4E).^[102] However, not all adhesion-promoting peptides are beneficial for tumor growth. While IKVAV and GFOGER promote tumor proliferation, it is often observed that YIGSR is associated with tumor-inhibitory effects.^[103] Together, the idea of adhering PDE onto or to the surrounding matrix has not been explored and is currently part of ongoing work in our laboratory. Besides the type of ECM component, it might also be worth

considering the concentration and spatial distribution of the ECM moiety presented; while it may be desired to adhere the explant down, matrix adhesivity may also encourage undesired migration of cells out from the explant, thereby leading to loss of tissue composition.

3.1.4. Lack of Standardized PDE Culture Media

The purpose of cell culture media is to provide essential nutrients and growth factors, maintain proper pH, and regulate osmotic pressure within the cultured cells and tissues. For most reported PDE cultures, cell culture media formulations that are well established for 2D monolayer and organoid cultures have been extrapolated for use in PDE cultures.^[32] While a systemic comparison of different cell culture media formulations in the context of PDE culture is necessary to determine the optimized formulation that can maintain PDEs ex vivo, a growing body of evidence suggests that the addition of tissue-specific supplements improves the longevity of explants ex vivo. For instance, the use of intestine-specific cell culture medium containing epithelial growth factor (EGF), Noggin, and R-spondin, significantly enhanced tissue viability and better retained the architecture of intestinal slices.^[104] In a similar vein, using HNSCC-specific medium that was modified from basal DMEM to Ham's F12 by the addition of insulin and EGF, Lee et al. successfully retained the viability of HNSCC-derived PDE cultures for 10 days, longer than the 2–6 days reported for HNSCC cultured in basal medium in the absence of additional supplements.^[50] Elevated insulin level has been linked to tumorigenesis and increased cancer growth,^[105] and EGF is known to promote cancer proliferation and also inhibit apoptosis in a number of different cancers, including NSCLC, HNSCC, CRC, breast cancer, and glioblastoma.^[106] Indeed, the presence of EGF and insulin was found to account for the improved lifespan of breast PDE as compared to those cultured in basal medium.^[43] Gastrin and fibroblast growth factor 10 (FGF10) have been shown to promote the growth of gastrointestinal tumor organoids.^[107] Given the known role of these supplements, they are likely to similarly support gastrointestinal PDE culture. Lastly, the provision of antioxidants, such as disphenyl diselenide instead of N-acetylcysteine or pycnogenol, was shown to provide additional growth support to PDAC tumor slices.^[108]

In addition to adding defined growth factors or supplements, it has been reported that human serum is advantageous over commonly used fetal bovine serum (FBS) for supporting PDE culture.^[108] Specifically, in the CANScrip platform, the use of autologous serum with tumor-matched ECM resulted in enhanced preservation of PDE as compared to the controls.^[109] Due to the inherent heterogeneity in the soluble environment of different cancer types, it would be extremely challenging to establish a standardized recipe for PDE culture. While the approach of leveraging organoid cell culture media formulations for PDE cultures is logical and could potentially work,^[110] less could be more. The addition of exogenous soluble factors to PDE cultures with intact stromal composition may mask certain cell–cell interactions and create culture artifacts. Hence, caution should be taken when formulating cell culture media for PDE cultures.

3.2. Use of Simplistic Readouts for PDE Characterization and Drug Response

The power of PDE lies in its potential ability to preserve cancer and stromal heterogeneity. By heterogeneity, this refers to the presence of subpopulations that may arise from genetic or non-genetic causes. For example, different tumoral niches that make up the tumor architecture may contribute to heterogeneity in cancer and stromal cell states. However, to date, the majority of reports have mostly leveraged simple histological analysis of PDE morphology, global viability readouts, and typically only use a few markers to characterize explant viability and composition over time in culture. Although recent reports have begun to more deeply characterize the complex ecosystem that exists within tumors to elucidate compositional changes in PDE during culture, these still lack the necessary resolution to reveal changes in subpopulation proportions. This is especially important if these models were to be used to assess the effect of immunotherapies. In this section, we will discuss how single-cell technologies can be leveraged to deeply interrogate and characterize PDE cultures.

3.2.1. Single Cell Technologies for Characterizing PDE Composition

Sequencing an entire transcriptome at the single-cell level, also known as single cell-RNA sequencing (scRNAseq), can be leveraged to perform deep characterization of PDE cultures and complement existing characterization methods. With scRNAseq, it is now possible to study how intra-tumoral heterogeneity translates into tumor-specific drug responses across multiple patients ex vivo. In a study where glioblastoma PDE was maintained using PTFE membrane inserts, scRNAseq led to discovery of cell type-specific responses to panobinostat, a histone deacetylase (HDAC) inhibitor. Specifically, panobinostat was found to selectively suppress the growth of a small subpopulation of cancer cells which overexpressed TOP2A and MK167. By comparing the PDE model to glioma spheres (GS), a commonly used glioblastoma 3D model, LeBlanc et al. found that PDE embedded into Matrigel was better at retaining heterogeneity of the tumors.^[111] In contrast to GS which tended to converge to one or two transcriptional state(s), Matrigel-based PDE fully retained the six states found in tumors.^[111] This finding highlights the superiority of PDE models over conventional reductionist models based on 3D spheres or organoids. In a similar vein, scRNAseq enabled stratification of different subclasses of EGFR-mutated lung adenocarcinoma.^[112] These distinct subtypes are differentiated by genetic features related to hypoxia, glycolysis, cell metabolism, cell cycle, and antigen presentation (**Figure 5A**).^[112]

Besides scRNAseq, single-cell analysis can also be achieved using CO-Detection by indEXing (CODEX), a highly multiplexed microscopy that permits spatially resolved identification of single cells. This imaging-enabled multiplexed characterization at the single cell level led to discovery of the heterogeneous response of immune cells to anti-CD47 and anti-PD-1.^[28c] The spatial reorganization of immune cells at the tumor core, not periphery, was observed for the first time with ICI treatment. However, while CODEX provides spatial information, this method does not support subclustering of cells (e.g., macrophages) as well as

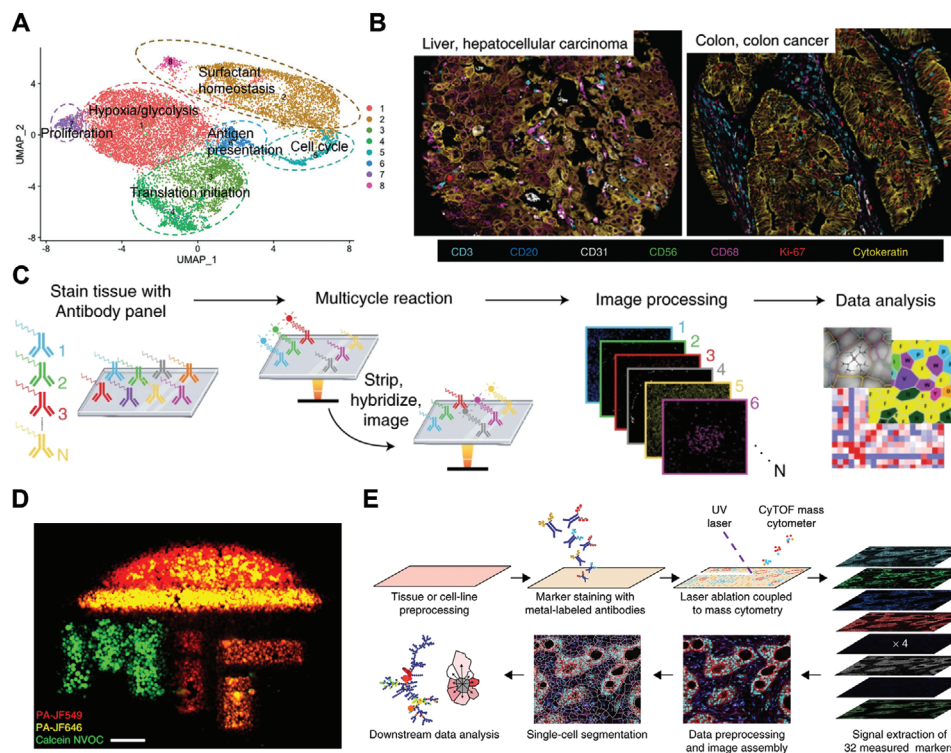


Figure 5. A) UMAP plots of 14,456 malignant cells display 8 subclasses with distinct expression signatures including hypoxia/glycolysis, oxidative phosphorylation, translation, cell cycle, antigen presentation, and proliferation. Reproduced with permission.^[112] Copyright 2021, Springer Nature. B) Representative images of hepatocellular carcinoma and colon cancer imaged with CODEX, highlighting seven markers — CD3, CD20, CD31, CD56, CD68, Ki-67, and cytokeratin — that are colored according to the bottom panel. Scale bar = 200 μ m. Reproduced with permission.^[114] Copyright 2021, Springer Nature. C) Schematic of the key steps in the CODEX imaging technology to achieve multiplexing IF on one sample. In brief, FFPE tissue samples are stained with the antibody panel followed by a multicycle reaction, that is iteratively imaging up to three antibodies and a nuclear stain per cycle, chemical stripping, hybridizing, and re-imaging for all antibodies in the panel. After that, raw images are computationally processed, and data analysis is performed. Reproduced with permission.^[114] Copyright 2021, Springer Nature. D) A representative image that shows a monolayer of HEK293T cells with selective subpopulations stained with various dyes using SPACECAT technology. 5-color encoding is achieved by sequential addition of 3 photoactivatable probes (calcein NVOC, PA-JF549, PA-JF646) and leveraging different photoactivation thresholds (10 s for calcein NVOC, 0.5 s for PA-JF549 and PA-JF646). Scale bar = 100 μ m. Green: uncaged calcein NVOC; yellow: uncaged PA-JF646, red: uncaged PA-JF549. Multiplexed encoding scheme repeated two times. Reproduced with permission.^[118] Copyright 2021, Springer Nature. E) Workflow of multiplexed imaging by CyTOF mass cytometry. Reproduced with permission.^[126] Copyright 2014, Springer Nature.^[112,114,118,126]

scRNAseq. In sum, the incorporation of scRNAseq technologies to deeply characterize complex PDE cultures will greatly accelerate the use of PDE cultures for drug testing. For example, by elucidating how long PDE cultures can maintain various cancer and immune cell subpopulations *ex vivo*, this information can be used to determine the ideal duration for evaluating ICIs. The use of cell-cell communication algorithms, such as NicheNet and CellPhoneDB, when characterizing these PDE cultures may also shed light on the crosstalk that occurs in tumors following drug perturbation.^[113] This would be highly useful especially for stromal-targeting therapeutics.

3.2.2. Spatial Technologies for Characterizing Cell–Cell Interactions

The unique ability of PDE to capture the original human TME *ex vivo* potentially provides an opportunity to understand how location within the TME and cell–cell interactions affect cancer progression and drug response. Yet, integration of spatial technologies, such as spatial transcriptomics or multiplex im-

munofluorescence (mIF), with PDE cultures is still rare. One potential technology that could be leveraged is CODEX, as described above,^[28c] which enables simultaneous staining of up to 60 markers *in situ* and deep investigation into the spatial relationship between single cells (Figure 5B,C).^[114] In another approach, a dual-panel mIF imaging system was developed to enable colocalization of PD-L1 expression on cancer cells, macrophages, and T cells in tumor slices of various cancer types.^[115] Interestingly, using mIF to spatially profile immune markers, it was found that Nivolumab increased the distance between effector T cells and regulatory T cells in melanoma PDE.^[11] In other methods, matrix-assisted laser desorption/ionization mass spectrometry (MALDI MS) is able to map small molecules in intact tissue samples, such as peptides and drugs, thereby providing opportunities for researchers to study drug trafficking within the tumor tissue.^[116] However, similar to CODEX, this technology is not compatible with live tissues. As these methods generally required fixed tissues, only a snapshot of cellular processes can be obtained from the PDE cultures.

On this note, the majority of studies leveraging PDE cultures make use of destructive end-point readouts, such as immunohistochemistry (IHC)/immunofluorescence (IF), and global viability or gene expression analyses, which provide minimal spatiotemporal information. The use of spatiotemporal technologies for the characterization of PDE cultures is currently underexplored; the use of which may enable the derivation of highly valuable information from these complex cultures. As an example, separate labeling of different cell types with non-toxic and photostable quantum dots (QD) tethered with different fluorophores has been used to study the spatiotemporal organization dynamics of PDOs.^[117] In another interesting development, live staining of a user-defined area within live cell cultures, which is enabled by spatially photo-activatable color encoded cell address tags, also known as SPACECAT, when integrated with cell-sorting techniques (i.e., FACS), is able to dissect complex spatial heterogeneity with up to 6 distinct regions within tissues (Figure 5D).^[118] The authors validated this technology in a mouse-derived lung adenocarcinoma model, and found that cell clusters at the periphery of the tumor differed significantly in the abundance of myeloid cells as compared to the tumor core. Specific cell types can also be live-imaged by tagging them with targeted probes. For instance, Kantelhardt et al. reported a EGFR-targeted probe to specifically distinguish glioma cells from normal cells in brain tissues.^[119] Vital staining of T and B cells in lymph node tissues has also been achieved.^[120] Although live tracking of multiple cell types within PDE cultures remains challenging, advances in spatiotemporal technologies and cell labeling may eventually allow for dynamic studies, unlocking much more information from these cultures which may be limited in availability.

3.3. Low Throughput Nature of PDE

Another key limitation of PDEs is the limited amount of tumor tissue available for processing into samples for drug testing. The amount of tissue that is available depends on the cancer type, treatment algorithm employed, and degree of necrosis. In instances where only biopsies are available, this problem is compounded. In most instances, as the amount of tissue is limited, drug testing can only be carried out in a low throughput manner. Here, we describe several technologies that can potentially enhance the throughput of PDE models.

3.3.1. Generate More PDE Slices/Fragments

Increasing the number of slices/tumor fragments obtained from the resected or biopsied tumor tissue is the most straightforward approach to increase the throughput of PDE cultures. This can potentially be achieved by increasing the number of samples generated per slice, or reducing the thickness of each slice. In an interesting approach, Horowitz et al. demonstrated the use of tissue choppers to create hundreds of 'cuboids' from a tissue slice,^[121] thereby greatly increasing the throughput of slice cultures. However, it is likely that in cancer types where there is high intra-tumoral heterogeneity in tumor composition, these 'cuboids' may have to be combined together to recapitulate the

variation in tumor composition within the same tumor. Rather than increase the number of samples by microdissection, it is also possible to increase the number of samples per tumor by decreasing slice thickness. While vibrating microtomes are widely used for tumor slicing, it is generally difficult to generate slices below 150 μm due to technical constraints and handling difficulties. As an alternative, laser microtomes that approach tissue in a non-contact manner can enable precise cutting of fresh tissues, with thicknesses ranging from 5 to 100 μm .^[122] Laser microtomes employ picosecond/femtosecond lasers which emit light in the near-infrared range,^[123] cutting tissues by inducing impulsive heat deposition at a ultra-fine spot (few μm) within the sample without causing collateral damage to peripheral tissues. Successful preparation of connective tissue slices with a thickness of 30 μm by laser cutting has been reported by Kunert-Keil et al.^[71a] In another study, Menne et al. used femtosecond laser microtomes to generate 10–20 μm porcine cornea, lung, and cartilage slices.^[71b] Tissue slices that were prepared by laser microtome for histological staining have also been reported.^[124] Although laser slicing has not been used for PDE research, we envision this technology will gain increasing traction and greatly accelerate the bench-to-bedside translation of PDE by increasing the throughput for drug testing.

3.3.2. Use of Multiplexed Assays on PDE Cultures

Besides generating more samples per tumor, the throughput of PDE models can potentially be improved by using multiplexed assays for sample characterization and drug testing. Conventional IHC typically only allows for the labeling of a single marker per tissue section. To extract more information per sample, multiplexing technologies can be used, such as cyclic immunofluorescence (IF), tyramide-based mIHC/mIF, and epitope-targeted mass spectrometry. CODEX, as described above, is a newly developed cyclic IF technology that allows up to 60 markers to be detected in one tissue section.^[128c] Lim et al. reported an automated staining protocol that incorporated tyramide signaling amplification (TSA) into IF technology, allowing simultaneous detection of 7 markers in human tissue sections.^[125] In another study, integrating IHC with cytometry by time of flight (CyTOF) mass cytometry led to simultaneous imaging of 32 proteins in a tissue sample (Figure 5E).^[126] Using human breast cancer samples as a proxy, Giesen et al. demonstrated the capability of this technology to stratify the subpopulations of tumor tissues and interrogate tumor heterogeneity and complex cell–cell interactions.^[126] For more information on recent developments in multiplex technologies, the reader can refer to other excellent reviews.^[127]

Tumor-on-a-chip microfluidic platforms may also greatly improve the throughput of PDE cultures by enabling the screening of multiple drugs on a single explant sample. Such a drug screening platform was first reported by Chang et al. for drug delivery to patient-derived brain slices.^[59] The devised microfluidic chip was reported to have 80 parallel open channels, allowing the simultaneous administration of different drug combinations to distinct parts of the same tissue. This smart microfluidic device was later adopted by Horowitz et al. with modifications for drug screening of human glioblastoma and colorectal tumor slices.^[128] By changing the base material from PDMS to PMMA, the newer

device enabled greater cost-effectiveness, precision, and higher-throughput (up to 40 drugs per device) for drug testing. However, it remains to be seen whether this approach would be feasible in cases where there is high intra-tumoral heterogeneity in tumor composition. Alternatively, it would be interesting to have a microfluidic system that allows testing of a set of drug combinations or drugs with a gradient of concentrations on the same tissue in a sequential manner. Although it has not been explored in tumor slices, recent advancements in microfluidics technology have proved it possible in the setting of single cells. For instance, Sun et al. developed a microfluidic chip platform with triangle-like laminar diffusion channels, allowing the sequential administration of different combinations of two drugs, paclitaxel, and cisplatin, to lung cancer cells.^[129] Another study by Eduati et al. reported a plug-based microfluidic system, which can also achieve sequential drug treatment by controlling braille valves (as plugs) to rapidly switch between 16 microchannels that contain various types of drug solutions.^[130] Other salient microfluidic designs for combinatorial drug treatments on single cells have been summarized elsewhere.^[131] These landmark studies may serve as a good reference to guide future exploration of high-throughput and sequential drug testing on tumor slices.

3.3.3. Use of Non-Destructive Assays on PDE Cultures

Current approaches to characterize PDE samples often require samples to be destroyed for downstream processing. As a result, multiple replicates are required, especially if characterization is performed at multiple time-points. Assays that are non-invasive to PDE tissues and permit multiplexed readouts on the same sample are thus valuable to enhance the throughput of the model. Most often, to measure tissue viability, MTT or luminescence-based ATP detection (e.g., CellTiter-Glo 3D) assays are used, where samples are destroyed by solubilization agents or mechanical means to generate readouts. Xing et al. developed a label-free metabolic assay that can enable live monitoring of cell viability in tumor slices for up to 7 days. In this approach, a caspase-3 reporter sensor C3 that expresses the CFP-Asp-Glu-Val-Asp (DEVD)-YFP protein was first introduced to the cancer cells followed by implantation into nude mice to form tumoroids.^[132] To make use of this approach for PDE cultures, further development is needed to ensure targeted delivery of the reporter to cancer cells within the tissue explant. In addition to genetic tagging, metabolic assays based on resazurin salts can potentially be used to measure PDE viability in a non-destructive manner.^[133] It should be noted that while long-term incubation of tissue samples with resazurin salts can potentially allow for live monitoring of cell viability, it is unclear how long-term exposure can affect the cell/tissue phenotype.^[134] To avoid this, time-lapse measurement of tumor viability should be performed, where resazurin salts are added only at designated time points and removed after the readout is acquired.^[134] Alternatively, recent developments in viability assays including RealTime-Glo MT Cell Viability Assay and CellTox Green Cytotoxicity Assay allow for time-lapse analysis of cell viability for up to 3 days.^[135] However, it is unclear whether these reagents are suitable for longer-term (> 3 days) monitoring of cell viability. Lastly, to overcome the need for fixation to process samples for histology, live-tracking of cancer cells

in human tumor tissues, as described above, can be achieved by using cancer-specific probes.^[119] Live-tracking of T and B cells has also been achieved by using anti-B220/CD45R and mitogenic anti-CD3 antibodies.^[120] However, it remains challenging to develop technologies enabling live and targeted tracking of other stromal cell types, including CAFs and endothelial cells. In seeking to elucidate the role of endothelial-to-mesenchymal transition (EndMT) in liver fibrosis development, a fluorescent reporter construct (EndMT-Rep) that specifically binds to endothelial cells was recently developed by Whiteford et al. to enable live-tracking of EndMT.^[136] In their approach, although HUVEC cells undergoing EndMT had significantly higher fluorescent signals, wild-type HUVEC cells were also tagged by EndMT-Rep. This may provide a useful future direction to engineer a pan-endothelial cell tracking system for studies involving PDE culture.

3.4. PDE as an Isolated System

Tumors grow in the context of an existing tissue or organ, connected to other tissues and organs in the body through the systemic circulation. One of the key limitations of current PDE cultures is the lack of integration of the explant with the circulatory system. The vasculature within tumors supports tumor growth, without which, necrosis is typically observed in vivo.^[137] This is likely one of the most important contributing factors to poor long-term PDE viability ex vivo. Additionally, tumors are linked to lymph tissue, where bidirectional immune cell trafficking occurs.^[138] In this section, we highlight potential strategies that can be undertaken to recreate the extra-tumoral microenvironment.

3.4.1. Promote PDE Vascularization

Vascularization of PDE not only enables perfusion to overcome hypoxia, but may also enable recapitulation of the intricate crosstalk between tumor and vascular endothelial cells. One way to achieve this is by engineering a co-culture system that allows tumor explants to be grown on vascular beds comprising endothelial cells as well as smooth muscle cells (SMCs). As an example, Bazou and Munn developed a pre-vascularized culture system for ex vivo maintenance of PDE derived from human melanoma and breast cancer xenografts.^[64b] With the support of lumenized vascular structures, the PDE cultures not only retained their morphology but also increased in size by 40% over a 10-day duration. To confirm these findings with patient samples, the authors used the same set-up on patient-derived pancreatic (PANC-1) PDE.^[64a] By comparing the pancreatic signature gene expression (cytokeratin-19, α -SMA, PDGFR α) in the PANC-1 explants after 10-days of ex vivo culture to that of freshly resected counterparts, the authors found that their model was able to not only maintain the viability of the explants, but also tumor-specific characteristics at the transcript level. Furthermore, preliminary drug testing performed on the explants identified that this vascular bed-supported tumor explant model better mimicked chemosensitivity of the original tumor in vivo, as compared to explants cultured in the absence of a vascular bed. In contrast, lack of vascular support led to significant dispersion of cells

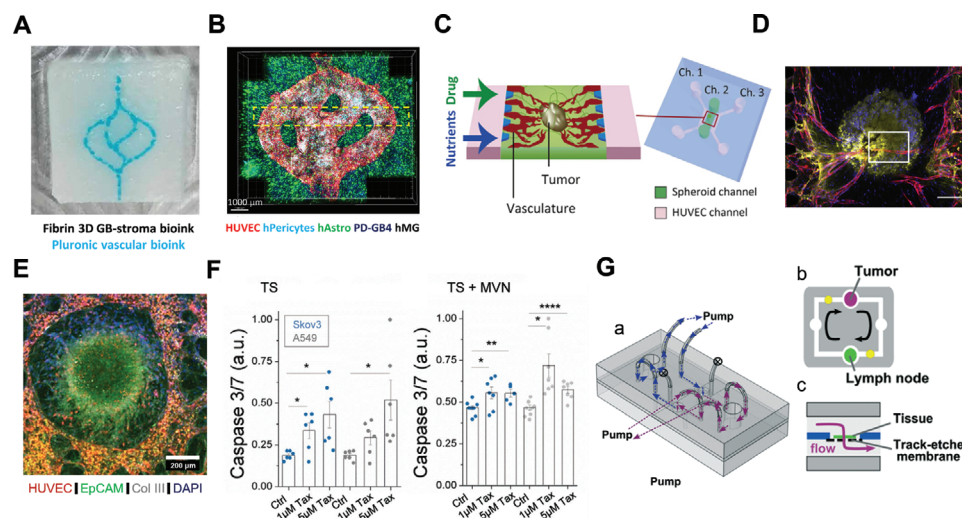


Figure 6. A) A 3D-printed cell-laden matrix containing pluronic-based vascular bioink (cyan) which is on top of the layers of fibrin 3D glioblastoma (GB)-stroma bioink (white). Reproduced with permission.^[141] Copyright 2021, American Association for the Advancement of Science (AAAS). B) Tiled Z-stack confocal microscopic image of the 3D-printed vascularized GB model. Blood vessels are lined with iRFP-labeled hPericytes (cyan) together with mCherry-labeled HUVEC (red) and surrounded by azurite-labeled PD-GB4 (GB, in blue), GFP-labeled hAstro (astrocytes, in green), and non-labeled hMG (microglia). The dashed box represents a coronal cross-sectional plane of the vessel.^[141] C) Schematic of vascularized cancer on a microchip model. Reproduced with permission.^[142] Copyright 2020, Elsevier. D) Representative immunofluorescence image of a tumor spheroid with the vasculature. Scale bar = 200 μ m. Reproduced with permission.^[142] Copyright 2020, Elsevier. E) Max-projection image of A549 (lung) tumor spheroid in a vascularized model. Tumor was fixed at day 7 and stained for EpCAM (green) and Collagen III (grey). Reproduced with permission.^[144] Copyright 2020, Wiley-VCH GmbH. F) Caspase 3/7 expression in skov3 (ovarian) and A549 (lung) tumor spheroids after 72 h treatment with paclitaxel (Tax) at various concentrations. Measurements were performed at day 10 in culture. Data were obtained from triplicate experiments. Mean \pm SEM is shown. Significant difference from control is indicated as * ($p < 0.05$), ** ($p < 0.01$), *** ($p < 0.001$), and **** ($p < 0.0001$). Reproduced with permission.^[144] Copyright 2020, Wiley-VCH GmbH. G) Schematic of the device operation for ex vivo co-culture of tumor and lymph node tissues. a) The flow path for recirculating fluid flow. b) Top view and c) side view of the co-culture microchip device. Tissue slices are placed on the track-etched membrane and fluid passes through the tissue slices when circulating in the device. Reproduced with permission.^[147] Copyright 2019, Royal Society of Chemistry.^[141,142,144,147]

and disintegration of the tumor core, making the tissues poorly amenable for drug evaluation.

Vascular constructs can also be fabricated using 3D bioprinting technologies. In this case, endothelial cells and/or stromal cells (SMCs, pericytes) are suspended in hydrogels consisting of alginate, HA, chitosan, fibrin, PEG, or gelatin, or a combination of two biomaterials or more.^[139] This cell-gel mixture is then printed by extrusion-based, inkjet-based, or laser-assisted bioprinters, and undergoes physical or chemical crosslinking to form the designated shape/pattern.^[140] Sacrificial hydrogels can be added to the printing formulation to allow special vascular conduits to form within the base hydrogel. In one example, Neufeld and Satchi-Fainaro leveraged 3D printing to enable complex tubular blood vessels to form adjacent to the glioblastoma (GB) core (Figure 6A,B).^[141] The 3D-printed blood vessels were constructed by embedding endothelial cells (HUVECs) in the sacrificial hydrogel comprising Pluronic F127 and thrombin (Th). In contrast to the 2D monolayer cultures, this 3D vascularized microenvironment better retained GB markers and reflected inter-patient heterogeneity in drug response. In another example, a single organoid was cultured in a microchannel where both sides of the inner wall comprised compact HUVEC layers (Figure 6C,D).^[142] Instead of a single organoid, this set-up could potentially be extrapolated for the culture of single PDE fragments. However, there is absence of an integrated vasculature in this system.

To integrate the existing vasculature within the PDE to the surrounding engineered vascular system, it is possible to vascularize the tissue itself using microfluidic systems.^[143] Microfluidic platforms outperform conventional tissue models by creating highly controllable environments to incorporate and monitor complex cell–cell and cell–environment interactions. For example, by encapsulating tumor spheroids and endothelial cells within a fibrin hydrogel placed within a microfluidic device, vascularization of the spheroid from all directions can be achieved (Figure 6E).^[144] Importantly, compared to the mono-cultures, enhanced resistance to paclitaxel was observed in the co-culture setting (Figure 6F).^[144] Microfluidic systems with incorporated self-assembled vascular networks were also recently reported by Boussommier-Calleja et al. and Song et al.^[145] Their approaches likewise involved injecting hydrogel solutions containing endothelial cells into the microfluidic device to allow spontaneous formation of complex vascular structures. With this setup, tumor infiltration and cancer-killing effects of immune cells (i.e., monocytes and NK cells) were investigated.

In sum, the incorporation of perfused blood vessels to artificially support PDE ex vivo is an attractive idea, particularly if doing so can also enable the preservation of the original vascular system within the PDE itself. However, there are key considerations to be made, including the life-span of these engineered vascular systems, the cell source for constructing these blood vessels in vitro (are conventionally used HUVECs appropriate?), and

lastly, the complexity of setting up such artificial vascular systems has to be balanced against throughput.

3.4.2. Leverage Lab-on-Chip Technologies for Integration of PDE with Other Tissues

In seeking to test ICIs such as anti-CTLA-4 using PDE cultures, besides vessels or engineered conduits that allow T-cell migration into the tumor explant, it would be necessary to have lymph nodes associated with the tumor tissue connected to the specimen. Lymph nodes play an important role in T-cell priming and the mechanism-of-action of CTLA-4 blockade.^[146] The tumor-associated lymph nodes may provide newly primed and peripherally expanded effector T-cells to the tumor tissue, thus contributing to the immune landscape of the tumor. In an attempt to include lymph tissue, Shim and Pompano leveraged an in-house modular microfluidic system to co-culture live murine lymph node tissue with tumor slices (Figure 6G).^[147] The tumor slices were kept alive on a porous membrane support (pore size 2 μm) for at least 24 h in the microfluidic chamber with medium recirculated in the device and passed through the samples. Interestingly, immune suppression was observed when lymph node slices were co-cultured with the tumor tissue but not healthy tissues, suggesting the ability of this microfluidic system to recapitulate communication between lymph node and tumor. While challenging, where both tumor and lymph nodes can be resected from the patient, PDEs can be established for both tissue types to set up a microfluidics-based co-culture system enabling the evaluation of ICIs such as CTLA-4 inhibitors. Beyond lymph tissue, given the advances in microfluidic systems and the ability to link multiple tissues or organs by vascular flow, it would be interesting to link PDE to other tissues and organs, such as the liver to recapitulate drug metabolism in vivo, or to other potential organ sites to mimic and understand metastasis.

4. Future Perspectives

The advent of single-cell and spatial technologies in recent years has created paradigm shifts in our understanding of tumor architecture and heterogeneity in the tumor stromal compartment. It is now clear that the composition of tumors is far more complex than was previously understood, where stromal cells (CAFs, immune cells, endothelial cells, etc.) within the same tumor exist in different states and potentially are spatially and functionally distinct.^[148] In taking the reductionist approach to model after such cancer types, several challenges loom ahead. For example, how do we go about isolating, maintaining, and/or expanding these different stromal cell states in vitro? How do we place these different cell types and subtypes in a patient-specific, in vivo-like spatial arrangement that maintains their state while recapitulating their crosstalk in vivo? How do we recapitulate heterogeneity in ECM type and orientation within the same tumor? These are important considerations as they have been implicated in response to therapy, especially ICIs, where the immune contexture, that is, the spatial distribution and density of immune cells, is correlated to drug response. With these bottlenecks to be addressed, there is a recent revival in interest in holistic PDE cultures, especially for evaluating immunotherapies.^[3b,28a,b,65] The notion that

PDE cultures can potentially preserve the original tumor in its entirety is becoming highly attractive again for personalized drug testing, and recent studies already suggest that PDE cultures can be predictive of drug response in cancer patients.^[11,28b,c,109] Yet, the majority of reported PDE cultures still rely on culture systems developed decades ago.

In this Review, we highlight some of the key parameters that limit this model, and proposed strategies to potentially overcome these limitations. Some of these limitations can well be addressed by bioengineers, who already have the expertise extrapolated from the fields of biomaterials and tissue engineering, as well as engineered microfluidic systems. Optimization of the underlying support to maintain PDE cultures in terms of mechanical and/or biochemical properties may contribute to enhanced viability of these cultures for longer durations ex vivo. However, in using scaffolds to support PDE culture, it is important to consider potential cell efflux into the supporting matrix, and avoid overestimation of tissue viability. The incorporation of perfusion, whether by fluid flow or by engineered vasculature systems, can potentially overcome the problem of hypoxia, thereby prolonging the viability of PDE cultures ex vivo. Microfluidic systems in the form of organs-on-a-chip may enable integration of these tumor explants with other tissues and organs of interest, improving recapitulation of drug response and drug metabolism. To overcome the inherent low throughput nature of PDE cultures, multiplexed assays should be integrated into the PDE workflow, so that much more information can be extracted from these limited cultures. Global assays typically used to characterize PDE cultures, such as bulk RNA sequencing, may not provide enough depth of resolution to adequately derive meaningful information from these highly complex cultures. The integration of single-cell technologies equipped with bioinformatics-based algorithms (for discerning cell-cell communication networks) with PDE will likely contribute to huge advances in our mechanistic understanding of how the TME affects drug response and vice versa. Complementary to single-cell technologies, machine learning approaches may also provide additional tools for assessing drug efficacy using PDE cultures. Deep learning-based extraction of immune cell features, such as morphology, motility, and position, with algorithms derived from prior training using past (pre)clinical data, has proved effective for the identification of ICI combinations.^[149] Recently, Ao et al. devised a high-throughput microfluidic platform with T cell infiltration tracking ability, acquired through clinical data-driven deep learning method, for the evaluation of novel anti-PD1-based drug combinations.^[150] This opens up a new path in using machine learning coupled with advanced microfluidic systems to perform rapid drug screening. An overview of typically used algorithms for the evaluation of cancer-immune cell interactions can be found in a recent review by Parlato et al.^[69] Regarding clinical implementation, attention should be given to how ex vivo drug response data can be translated into physiologically relevant dosages in patients. Machine-learning platforms, such as quadratic phenotypic optimization platform (QPOP) and CURATE.AI, recently developed AI platforms for optimization of combination therapy, can potentially be used with PDE cultures to improve the clinical-decision making process on personalized drug dosage for each patient.^[151] Lastly, it is envisioned that biobanks of drug response derived from PDE cultures that

are deeply characterized for genomic and transcriptomic profiles as well as corresponding clinical response data, may present an unprecedented opportunity for predicting drug response in future cohorts of patients, especially for stromal-targeting drugs such as ICIs. Unlike organoid-based biobanks which are cancer cell-centric, PDE biobanks offer the opportunity to rapidly and accurately carry out ICI-based combination therapy trials ex vivo, rather than in actual clinical trials in patients.

In sum, interdisciplinary collaboration across oncology, materials science, microfluidic engineering, single-cell and imaging technologies, as well as tight collaboration with clinical collaborators, is indispensable for resurrecting PDE cultures. There is no better time to bring back PDE cultures to truly make personalized drug testing a reality, and we already have some of the engineering solutions and technologies in place to overcome key bottlenecks limiting their translation into the clinic.

Acknowledgements

E.L.S.F. would like to acknowledge funding from the National University of Singapore Start-Up grant (A-0009372-01-00), MOE Tier 1 grant (A-0009385-01-00), NUS R&G Post-Doctoral Fellowship (A-0000065-51-00), MOE Tier 2 grant (MOE-T2EP30221-0016) and the National Medical Research Council - Open Fund Individual Research Grant.

Conflict of Interest

The authors declare no conflict of interest.

Keywords

drug screening, in vitro tumor models, patient-derived tumor explants, personalized oncology, tumor microenvironments

Received: September 6, 2022

Revised: January 4, 2023

Published online: February 22, 2023

- [1] World Health Organization **2022**, <https://www.who.int/news-room/fact-sheets/detail/cancer>.
- [2] a) A. Haslam, J. Gill, V. Prasad, *Int. J. Cancer* **2021**, *148*, 713; b) E. B. Maldonado, S. Parsons, E. Y. Chen, A. Haslam, V. Prasad, *Future Sci. OA* **2020**, *6*, FSO600.
- [3] a) K. T. Flaherty, R. J. Gray, A. P. Chen, S. Li, L. M. McShane, D. Patton, S. R. Hamilton, P. M. Williams, A. J. Iafrate, J. Sklar, E. P. Mitchell, L. N. Harris, N. Takebe, D. J. Sims, B. Coffey, T. Fu, M. Routbort, J. A. Zwiebel, L. V. Rubinstein, R. F. Little, C. L. Arteaga, R. Comis, J. S. Abrams, P. J. O'Dwyer, B. A. Conley, N.-M. team, *J. Clin. Oncol.* **2020**, *38*, 3883; b) A. Letai, P. Bholia, A. L. Welm, *Cancer Cell* **2022**, *40*, 26.
- [4] M. Yao, P. Fu, *Chin. Clin. Oncol.* **2018**, *7*, 27.
- [5] M. Takeda, K. Nakagawa, *Curr. Cancer Drug Targets* **2015**, *15*, 792.
- [6] P. Schummer, B. Schilling, A. Gesierich, *Am. J. Clin. Dermatol.* **2020**, *21*, 493.
- [7] M. Abbaspour Babaei, B. Kamalidehghan, M. Saleem, H. Z. Huri, F. Ahmadipour, *Drug Des., Dev. Ther.* **2016**, *10*, 2443.
- [8] A. P. Chen, S. Kummar, N. Moore, L. V. Rubinstein, Y. Zhao, P. M. Williams, A. Palmisano, D. Sims, G. O'Sullivan Coyne, C. L. Rosenberger, M. Simpson, K. P. S. Raghav, F. Meric-Bernstam, S. Leong, S. Waqar, J. C. Foster, M. M. Konate, B. Das, C. Karlovich, C. J. Lih, E. Polley, R. Simon, M. C. Li, R. Piekarz, J. H. Doroshow, *JCO Precis. Oncol.* **2021**, *5*, 133.
- [9] J. Sands, S. J. Mandrekar, G. R. Oxnard, D. E. Kozono, S. L. Hillman, S. E. Dahlberg, Z. Sun, J. E. Chaft, R. Govindan, D. E. Gerber, J. E. Gray, S. M. Malik, M. M. Mooney, P. A. Janne, E. E. Vokes, K. Kelly, S. S. Ramalingam, T. Stinchcombe, *J. Clin. Oncol.* **2020**, *38*, TPS9077.
- [10] E. Fountzilas, A. M. Tsimberidou, *Expert Rev. Clin. Pharmacol.* **2018**, *11*, 797.
- [11] I. R. Powley, M. Patel, G. Miles, H. Pringle, L. Howells, A. Thomas, C. Kettleborough, J. Bryans, T. Hammonds, M. MacFarlane, C. Pritchard, *Br. J. Cancer* **2020**, *122*, 735.
- [12] S. Y. Choi, D. Lin, P. W. Gout, C. C. Collins, Y. Xu, Y. Wang, *Adv. Drug Delivery Rev.* **2014**, *79–80*, 222.
- [13] G. Gunaydin, *Front. Oncol.* **2021**, *11*, 668349.
- [14] S. M. Ridge, F. J. Sullivan, S. A. Glynn, *Mol. Cancer* **2017**, *16*, 31.
- [15] K. Hida, N. Maishi, D. A. Annan, Y. Hida, *Int. J. Mol. Sci.* **2018**, *19*, 1272.
- [16] H. Gonzalez, C. Hagerling, Z. Werb, *Genes Dev.* **2018**, *32*, 1267.
- [17] R. Baghban, L. Roshangar, R. Jahanban-Esfahlan, K. Seidi, A. Ebrahimi-Kalan, M. Jaymand, S. Kolahian, T. Javaheri, P. Zare, *Cell Commun. Signaling* **2020**, *18*, 59.
- [18] a) P. R. Prasetyanti, J. P. Medema, *Mol. Cancer* **2017**, *16*, 41; b) R. Ge, Z. Wang, L. Cheng, *npj Precis. Oncol.* **2022**, *6*, 31.
- [19] H. Zhao, L. Wu, G. Yan, Y. Chen, M. Zhou, Y. Wu, Y. Li, *Signal Transduction Targeted Ther.* **2021**, *6*, 263.
- [20] M. R. Junttila, F. J. de Sauvage, *Nature* **2013**, *501*, 346.
- [21] J. Winkler, A. Abisoye-Ogunniyan, K. J. Metcalf, Z. Werb, *Nat. Commun.* **2020**, *11*, 5120.
- [22] J. P. Gillet, S. Varma, M. M. Gottesman, *J. Natl. Cancer Inst.* **2013**, *105*, 452.
- [23] H. J. Burstein, P. B. Mangu, M. R. Somerfield, D. Schrag, D. Samson, L. Holt, D. Zelman, J. A. Ajani, *J. Clin. Oncol.* **2011**, *29*, 3328.
- [24] a) E. Driehuis, K. Kretzschmar, H. Clevers, *Nat. Protoc.* **2020**, *15*, 3380; b) S. N. Ooft, F. Weeber, K. K. Dijkstra, C. M. McLean, S. Kaing, E. van Werkhoven, L. Schipper, L. Hoes, D. J. Vis, J. van de Haar, W. Prevoo, P. Snaebjornsson, D. van der Velden, M. Klein, M. Chalabi, H. Boot, M. van Leerdam, H. J. Bloemendal, L. V. Beerepoot, L. Wessels, E. Cuppen, H. Clevers, E. E. Voest, *Sci. Transl. Med.* **2019**, *11*, eaay2574.
- [25] C. P. Sun, H. R. Lan, X. L. Fang, X. Y. Yang, K. T. Jin, *Front. Immunol.* **2022**, *13*, 770465.
- [26] G. Vlachogiannis, S. Hedayat, A. Vatsiou, Y. Jamin, J. Fernandez-Mateos, K. Khan, A. Lampis, K. Eason, I. Huntingford, R. Burke, M. Rata, D. M. Koh, N. Tunariu, D. Collins, S. Hulkki-Wilson, C. Ragulan, I. Spiteri, S. Y. Moorcraft, I. Chau, S. Rao, D. Watkins, N. Fotiadis, M. Bali, M. Darvish-Damavandi, H. Lote, Z. Eltahir, E. C. Smyth, R. Begum, P. A. Clarke, J. C. Hahne, et al., *Science* **2018**, *359*, 920.
- [27] C. Chen, W. Lin, Y. Huang, X. Chen, H. Wang, L. Teng, *J. Cancer* **2021**, *12*, 28.
- [28] a) P. Voabil, M. de Bruijn, L. M. Roelofsen, S. H. Hendriks, S. Brokamp, M. van den Braber, A. Broeks, J. Sanders, P. Herzig, A. Zippelius, C. U. Blank, K. J. Hartemink, K. Monkhorst, J. Haanen, T. N. Schumacher, D. S. Thommen, *Nat. Med.* **2021**, *27*, 1250; b) N. Gavert, Y. Zwang, R. Weiser, O. Greenberg, S. Halperin, O. Jacoby, G. Malle, O. Sandler, A. J. Berger, E. Stossel, D. Rotin, A. Grinshpun, I. Kamer, J. Bar, G. Pines, D. Saidian, I. Bar, S. Golan, E. Rosenbaum, A. Nadu, E. Ben-Ami, R. Weitzen, H. Nechushtan, T. Golan, B. Brenner, A. Nissan, O. Margalit, D. Hershkowitz, G. Lahat, R. Straussman, *Nat. Cancer* **2022**, *3*, 219; c) T. Shekarian, C. P. Zinner, E. M. Bartoszek, W. Duchemin, A. T. Wachnowicz, S. Hogan, M. M. Etter, J. Flammer, C. Paganetti, T. A. Martins, P. Schmassmann, S. Zanganeh, F. L. Goff, M. G. Muraro, M. F. Ritz, D. Phillips, S. S. Bhate,

- G. L. Barlow, G. P. Nolan, C. M. Schurch, G. Hutter, *Sci. Adv.* **2022**, 8, eabn9440.
- [29] a) T. K. T. Furukawa, R. M. Hoffman, *Clin. Cancer Res.* **1995**, 1, 7; b) R. A. Vescio, K. M. Connors, T. Kubota, R. M. Hoffman, *Proc. Natl. Acad. Sci. U. S. A.* **1991**, 88, 5163.
- [30] a) A. Yin, J. G. C. van Hasselt, H. J. Guchelaar, L. E. Friberg, D. Moes, *Sci. Rep.* **2022**, 12, 4206; b) G. Stein-O'Brien, L. T. Kagohara, S. Li, M. Thakar, R. Ranaweera, H. Ozawa, H. Cheng, M. Considine, S. Schmitz, A. V. Favorov, L. V. Danilova, J. A. Califano, E. Izumchenko, D. A. Gaykalova, C. H. Chung, E. J. Fertig, *Genome Med.* **2018**, 10, 37; c) S. Helfenstein, O. Riesterer, U. R. Meier, A. Papachristofilou, B. Kasenda, M. Pless, S. I. Rothschild, *Radiat. Oncol.* **2019**, 14, 32.
- [31] a) A. E. Freeman, R. M. Hoffman, *Proc. Natl. Acad. Sci. U. S. A.* **1986**, 83, 2694; b) J. Kokkinos, G. Sharbeen, K. S. Haghighi, R. M. C. Ignacio, C. Kopecky, E. Gonzales-Aloy, J. Youkhana, P. Timpson, B. A. Pereira, S. Ritchie, E. Pandzic, C. Boyer, T. P. Davis, L. M. Butler, D. Goldstein, J. A. McCarroll, P. A. Phillips, *Sci. Rep.* **2021**, 11, 1944; c) D. L. Holliday, M. A. Moss, S. Pollock, S. Lane, A. M. Shaaban, R. Millican-Slater, C. Nash, A. M. Hanby, V. Speirs, *J. Clin. Pathol.* **2013**, 66, 253.
- [32] A. R. Templeton, P. L. Jeffery, P. B. Thomas, M. P. J. Perera, G. Ng, A. R. Calabrese, C. Nicholls, N. J. Mackenzie, J. Wood, L. J. Bray, I. Vela, E. W. Thompson, E. D. Williams, *Front. Oncol.* **2021**, 11, 767697.
- [33] a) J. Leighton, *J. Natl. Cancer Inst.* **1951**, 12, 545; b) J. Leighton, G. Justh, M. Esper, R. L. Kronenthal, *Science* **1967**, 155, 1259.
- [34] I. Gris-Cardenas, M. Rabano, M. D. M. Vivanco, *Methods Mol. Biol.* **2022**, 2471, 301.
- [35] M. M. Centenera, T. E. Hickey, S. Jindal, N. K. Ryan, P. Ravindranathan, H. Mohammed, J. L. Robinson, M. J. Schiewer, S. Ma, P. Kapur, P. D. Sutherland, C. E. Hoffmann, C. G. Roehrborn, L. G. Gomella, J. S. Carroll, S. N. Birrell, K. E. Knudsen, G. V. Raj, L. M. Butler, W. D. Tilley, *Mol. Oncol.* **2018**, 12, 1608.
- [36] A. J. C. Dohmen, J. Sanders, S. Canisius, E. S. Jordanova, E. A. Aalbersberg, M. W. M. van den Brekel, J. Neefjes, C. L. Zuur, *Oncotargets Ther.* **2018**, 9, 25034.
- [37] M. M. Centenera, J. L. Gillis, A. R. Hanson, S. Jindal, R. A. Taylor, G. P. Risbridger, P. D. Sutherland, H. I. Scher, G. V. Raj, K. E. Knudsen, T. Yeadon, Australian Prostate Cancer BioResource, W. D. Tilley, L. M. Butler, *Clin. Cancer Res.* **2012**, 18, 3562.
- [38] H. Mohammed, I. A. Russell, R. Stark, O. M. Rueda, T. E. Hickey, G. A. Tarulli, A. A. Serandour, S. N. Birrell, A. Bruna, A. Saadi, S. Menon, J. Hadfield, M. Pugh, G. V. Raj, G. D. Brown, C. D'Santos, J. L. Robinson, G. Silva, R. Launchbury, C. M. Perou, J. Stingl, C. Caldas, W. D. Tilley, J. S. Carroll, *Nature* **2015**, 523, 313.
- [39] A. A. Shafi, M. J. Schiewer, R. de Leeuw, E. Dylgjeri, P. A. McCue, N. Shah, L. G. Gomella, C. D. Lallas, E. J. Trabulsi, M. M. Centenera, T. E. Hickey, L. M. Butler, G. Raj, W. D. Tilley, E. Cukierman, K. E. Knudsen, *Eur. Urol. Oncol.* **2018**, 1, 325.
- [40] a) M. M. Centenera, A. D. Vincent, M. Moldovan, H. M. Lin, D. J. Lynn, L. G. Horvath, L. M. Butler, *Cancers* **2022**, 14, 1708; b) J. L. Dean, A. K. McClendon, T. E. Hickey, L. M. Butler, W. D. Tilley, A. K. Witkiewicz, E. S. Knudsen, *Cell Cycle* **2012**, 11, 2756; c) J. Geller, L. Sionit, C. Partido, L. Li, X. Tan, T. Youngkin, D. Nachtsheim, R. M. Hoffman, *Prostate* **1998**, 34, 75; d) M. M. Centenera, G. V. Raj, K. E. Knudsen, W. D. Tilley, L. M. Butler, *Nat. Rev. Urol.* **2013**, 10, 483.
- [41] P. Dimou, S. Trivedi, M. Liousia, R. R. D'Souza, A. Klampatsa, *Antibodies* **2022**, 11, 26.
- [42] a) M. A. Kern, A. M. Haugg, E. Eiteneuer, E. Konze, U. Drebbler, H. P. Dienes, K. Breuhahn, P. Schirmacher, H. U. Kasper, *Liver Int.* **2006**, 26, 604; b) H. van der Kuip, T. E. Murdter, M. Sonnenberg, M. McClellan, S. Gutzeit, A. Gerteis, W. Simon, P. Fritz, W. E. Aulitzky, *BMC Cancer* **2006**, 6, 86; c) I. E. Carranza-Torres, N. E. Guzman-Delgado, C. Coronado-Martinez, J. I. Banuelos-Garcia, E. Viveros-Valdez, J. Moran-Martinez, P. Carranza-Rosales, *Biomed Res. Int.* **2015**, 2015, 618021.
- [43] K. A. Naipal, N. S. Verkaik, H. Sanchez, C. H. van Deurzen, M. A. den Bakker, J. H. Hoeijmakers, R. Kanaar, M. P. Vreeswijk, A. Jager, D. C. van Gent, *BMC Cancer* **2016**, 16, 78.
- [44] E. J. Davies, M. Dong, M. Gutekunst, K. Narhi, H. J. van Zoggel, S. Blom, A. Nagaraj, T. Metsalu, E. Oswald, S. Erkens-Schulze, J. A. Delgado San Martin, R. Turkki, S. R. Wedge, T. M. af Hallstrom, J. Schueler, W. M. van Weerden, E. W. Verschuren, S. T. Barry, H. van der Kuip, J. A. Hickman, *Sci. Rep.* **2015**, 5, 17187.
- [45] A. S. Nagaraj, J. Bao, A. Hemmes, M. Machado, K. Narhi, E. W. Verschuren, *J. Visualized Exp.* **2018**.
- [46] R. Sivakumar, M. Chan, J. S. Shin, N. Nishida-Aoki, H. L. Kenerson, O. Elemento, H. Beltran, R. Yeung, T. S. Gujral, *Oncoimmunology* **2019**, 8, e1670019.
- [47] J. J. Parker, P. Canoll, L. Niswander, B. K. Kleinschmidt-DeMasters, K. Foshay, A. Waziri, *Sci. Rep.* **2018**, 8, 18002.
- [48] E. J. Chadwick, D. P. Yang, M. G. Filbin, E. Mazzola, Y. Sun, O. Behar, M. F. Pazyra-Murphy, L. Goumnerova, K. L. Ligon, C. D. Stiles, R. A. Segal, *J. Visualized Exp.* **2015**, 105, e53304-1.
- [49] H. S. Leong, A. F. Chambers, *Proc. Natl. Acad. Sci. U. S. A.* **2014**, 111, 887.
- [50] J. Lee, J. H. You, D. Shin, J. L. Roh, *J. Cancer Res. Clin. Oncol.* **2020**, 146, 2497.
- [51] D. Dorigiv, K. Simeone, L. Communal, J. Kendall-Dupont, A. St-Georges-Robillard, B. Peant, E. Carmona, A. M. Mes-Masson, T. Gervais, *Cancers* **2021**, 13, 4208.
- [52] H. L. Kenerson, K. M. Sullivan, K. P. Labadie, V. G. Pillarisetty, R. S. Yeung, *STAR Protoc.* **2021**, 2, 100574.
- [53] R. de Hoogt, M. F. Estrada, S. Vidic, E. J. Davies, A. Osswald, M. Barbier, V. E. Santo, K. Gjerde, H. van Zoggel, S. Blom, M. Dong, K. Narhi, E. Boghaert, C. Brito, Y. Chong, W. Sommergruber, H. van der Kuip, W. M. van Weerden, E. W. Verschuren, J. Hickman, R. Graeser, *Sci. Data* **2017**, 4, 170170.
- [54] S. Abreu, F. Silva, R. Mendes, T. F. Mendes, M. Teixeira, V. E. Santo, E. R. Boghaert, A. Felix, C. Brito, *Sci. Rep.* **2020**, 10, 19462.
- [55] N. Ferrell, J. Cheng, S. Miao, S. Roy, W. H. Fissell, *ASAIO J.* **2018**, 64, 766.
- [56] C. Manfredonia, M. G. Muraro, C. Hirt, V. Mele, V. Governa, A. Papadimitropoulos, S. Daster, S. D. Soysal, R. A. Droezer, R. Mechera, D. Oertli, R. Rosso, M. Bolli, A. Zettl, L. M. Terracciano, G. C. Spagnoli, I. Martin, G. Iezzi, *Adv. Biosyst.* **2019**, 3, 1800300.
- [57] Z. Huo, R. Bilang, C. T. Supuran, N. von der Weid, E. Bruder, S. Holland-Cunz, I. Martin, M. G. Muraro, S. J. Gros, *Int. J. Mol. Sci.* **2022**, 23, 3128.
- [58] a) B. Altmann, C. Grün, C. Nies, E. Gottwald, *Processes* **2020**, 9, 21; b) K. Hattori, S. Sugiura, T. Kanamori, *Methods Mol. Biol.* **2014**, 1104, 251; c) T. Kwon, H. Prentice, J. Oliveira, N. Madziva, M. E. Warkiani, J. P. Hamel, J. Han, *Sci. Rep.* **2017**, 7, 6703.
- [59] T. C. Chang, A. M. Mikheev, W. Huynh, R. J. Monnat, R. C. Rostomily, A. Folch, *Lab Chip* **2014**, 14, 4540.
- [60] M. Astolfi, B. Peant, M. A. Lateef, N. Rousset, J. Kendall-Dupont, E. Carmona, F. Monet, F. Saad, D. Provencher, A. M. Mes-Masson, T. Gervais, *Lab Chip* **2016**, 16, 312.
- [61] C. C. Huang, W. T. Chia, M. F. Chung, K. J. Lin, C. W. Hsiao, C. Jin, W. H. Lim, C. C. Chen, H. W. Sung, *J. Am. Chem. Soc.* **2016**, 138, 5222.
- [62] G. Song, C. Liang, X. Yi, Q. Zhao, L. Cheng, K. Yang, Z. Liu, *Adv. Mater.* **2016**, 28, 2654.
- [63] S. Suvarnapathaki, X. Wu, D. Lantigua, M. A. Nguyen, G. Camci-Unal, *NPG Asia Mater.* **2019**, 11, 65.
- [64] a) D. Bazou, N. Maimon, G. Gruionu, J. Grahovac, G. Seano, H. Liu, C. L. Evans, L. L. Munn, *J. Tissue Eng. Regener. Med.* **2018**, 12, e318; b) D. Bazou, N. Maimon, G. Gruionu, L. L. Munn, *Integr. Biol.* **2016**, 8, 1301.

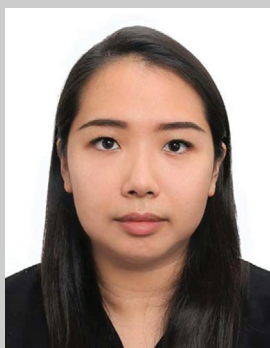
- [65] D. S. Thommen, V. H. Koelzer, P. Herzig, A. Roller, M. Trefny, S. Dimeloe, A. Kiialainen, J. Hanhart, C. Schill, C. Hess, S. Savic Prince, M. Wiese, D. Lardinois, P. C. Ho, C. Klein, V. Karanikas, K. D. Mertz, T. N. Schumacher, A. Zippelius, *Nat. Med.* **2018**, 24, 994.
- [66] X. Jiang, Y. D. Seo, J. H. Chang, A. Covelev, E. N. Nigeh, S. Pan, F. Jalikis, R. S. Yeung, I. N. Crispe, V. G. Pillarisetty, *Oncoimmunology* **2017**, 6, e1333210.
- [67] A. R. Aref, M. Campisi, E. Ivanova, A. Portell, D. Larios, B. P. Piel, N. Mathur, C. Zhou, R. V. Coakley, A. Bartels, M. Bowden, Z. Herbert, S. Hill, S. Gilhooley, J. Carter, I. Canadas, T. C. Thai, S. Kitajima, V. Chiono, C. P. Paweletz, D. A. Barbie, R. D. Kamm, R. W. Jenkins, *Lab Chip* **2018**, 18, 3129.
- [68] N. Moore, D. Doty, M. Zielstorff, I. Kariv, L. Y. Moy, A. Gimbel, J. R. Chevillet, N. Lowry, J. Santos, V. Mott, L. Kratchman, T. Lau, G. Addona, H. Chen, J. T. Borenstein, *Lab Chip* **2018**, 18, 1844.
- [69] S. Parlato, G. Grisanti, G. Sinibaldi, G. Peruzzi, C. M. Casciola, L. Gabriele, *Lab Chip* **2021**, 21, 234.
- [70] a) H. P. Behrsing, M. J. Furniss, M. Davis, J. E. Tomaszewski, R. E. Parchment, *Toxicol. Sci.* **2013**, 131, 470; b) X. Wu, J. B. Roberto, A. Knupp, H. L. Kenerson, C. D. Truong, S. Y. Yuen, K. J. Bremel, M. Tuefferd, A. Chen, H. Horton, R. S. Yeung, I. N. Crispe, *J. Immunol. Methods* **2018**, 455, 71.
- [71] a) C. Kunert-Keil, H. Richter, I. Zeidler-Rentzsch, I. Bleeker, T. Gredes, *Ann. Anat.* **2019**, 222, 153; b) Microtomy with Femtosecond Lasers, PEGGY MENNE, ROWIAK GMBH, **2007**, https://www.photonics.com/Articles/Microtomy_with_Femtosecond_Lasers/a38890.
- [72] M. E. Sherman, R. A. Vierkant, S. Kaggal, T. L. Hoskin, M. H. Frost, L. Denison, D. W. Visscher, J. M. Carter, S. J. Winham, M. R. Jensen, D. C. Radisky, C. M. Vachon, A. C. Degnim, *Cancer Prev. Res.* **2020**, 13, 967.
- [73] a) S. B. Lim, S. J. Tan, W. T. Lim, C. T. Lim, *Nat. Commun.* **2017**, 8, 1734; b) J. Huang, L. Zhang, D. Wan, L. Zhou, S. Zheng, S. Lin, Y. Qiao, *Signal Transduction Targeted Ther.* **2021**, 6, 153; c) K. M. Wisdom, K. Adebawale, J. Chang, J. Y. Lee, S. Nam, R. Desai, N. S. Rossen, M. Rafat, R. B. West, L. Hodgson, O. Chaudhuri, *Nat. Commun.* **2018**, 9, 4144.
- [74] C. Ricciardelli, N. A. Lokman, I. Sabit, K. Gunasegaran, W. M. Bonner, C. E. Pyragius, A. M. Macpherson, M. K. Oehler, *Cancer Lett.* **2018**, 421, 51.
- [75] Y. M. Jeong, C. Bang, M. Park, S. Shin, S. Yun, C. M. Kim, G. Jeong, Y. J. Chung, W. S. Yun, J. H. Lee, S. Jin, *Cells* **2021**, 10, 589.
- [76] K. E. Bailey, C. Pino, M. L. Lennon, A. Lyons, J. G. Jacot, S. R. Lammers, M. Konigshoff, C. M. Magin, *Am. J. Respir. Cell Mol. Biol.* **2020**, 62, 14.
- [77] M. Zhang, P. Boughton, B. Rose, C. S. Lee, A. M. Hong, *Int. J. Biomater.* **2013**, 2013, 396056.
- [78] Y. Takahashi, Y. Tabata, *J. Biomater. Sci., Polym. Ed.* **2004**, 15, 41.
- [79] B. B. Mandal, S. C. Kundu, *Biomaterials* **2009**, 30, 2956.
- [80] I. Bruzauskaitė, D. Bironaitė, E. Bagdonas, E. Bernotienė, *Cytotechnology* **2016**, 68, 355.
- [81] D. W. Hutmacher, T. B. F. Woodfield, P. D. Dalton, *Tissue Eng.* **2014**, 311, <https://doi.org/10.1016/B978-0-12-420145-3.00010-9>.
- [82] Q. L. Loh, C. Choong, *Tissue Eng., Part B* **2013**, 19, 485.
- [83] I. Buj-Corral, A. Bagheri, O. Petit-Rojo, *Materials* **2018**, 11, 1532.
- [84] a) X. Miao, D. Sun, *Materials* **2009**, 3, 26; b) H. Chen, Q. Han, C. Wang, Y. Liu, B. Chen, J. Wang, *Front. Bioeng. Biotechnol.* **2020**, 8, 609.
- [85] a) N. Gjorevski, N. Sachs, A. Manfrin, S. Giger, M. E. Bragina, P. Ordóñez-Moran, H. Clevers, M. P. Lutolf, *Nature* **2016**, 539, 560; b) A. J. Engler, S. Sen, H. L. Sweeney, D. E. Discher, *Cell* **2006**, 126, 677.
- [86] a) M. Sylvestre, C. A. Crane, S. H. Pun, *Adv. Mater.* **2020**, 32, 1902007; b) Y. Zhu, Q. Zhang, X. Shi, D. Han, *Adv. Mater.* **2019**, 31, 1804950; c) R. S. Stowers, S. C. Allen, L. J. Suggs, *Proc. Natl. Acad. Sci. U. S. A.* **2015**, 112, 1953; d) C. Wang, S. Sinha, X. Jiang, L. Murphy, S. Fitch, C. Wilson, G. Grant, F. Yang, *Tissue Eng., Part A* **2021**, 27, 390.
- [87] E. A. Aisenbrey, W. L. Murphy, *Nat. Rev. Mater.* **2020**, 5, 539.
- [88] L. Varinelli, M. Guaglio, S. Brich, S. Zanutto, A. Belfiore, F. Zanardi, F. Iannelli, A. Oldani, E. Costa, M. Chighizola, E. Lorenc, S. P. Minardi, S. Fortuzzi, M. Filugelli, G. Garzone, F. Pisati, M. Vecchi, G. Pruneri, K. Shigeki, D. Baratti, L. Cattaneo, D. Parazzoli, A. Podestà, M. Milione, M. Deraco, M. A. Pierotti, M. Gariboldi, *bioRxiv* **2021.07.15.452437** **2021**.
- [89] S. Sasikumar, S. Chameettachal, B. Cromer, F. Pati, P. Kingshott, *Curr. Opin. Biomed. Eng.* **2019**, 10, 123.
- [90] J. Jang, T. G. Kim, B. S. Kim, S. W. Kim, S. M. Kwon, D. W. Cho, *Acta Biomater.* **2016**, 33, 88.
- [91] a) K. E. Drzewiecki, A. S. Parmar, I. D. Gaudet, J. R. Branch, D. H. Pike, V. Nanda, D. I. Shreiber, *Langmuir* **2014**, 30, 11204; b) C. Liu, D. Lewin Mejia, B. Chiang, K. E. Luker, G. D. Luker, *Acta Biomater.* **2018**, 75, 213; c) S. Moscato, F. Ronca, D. Campani, S. Danti, *J. Funct. Biomater.* **2015**, 6, 16; d) T. Jiang, J. Munguia-Lopez, S. Flores-Torres, J. Grant, S. Vijayakumar, A. De Leon-Rodriguez, J. M. Kinsella, *J. Visualized Exp.* **2018**, 137, e57826-1; e) A. Takahashi, Y. Suzuki, T. Suhara, K. Omichi, A. Shimizu, K. Hasegawa, N. Kokudo, S. Ohta, T. Ito, *Biomacromolecules* **2013**, 14, 3581; f) M. Mihajlovic, L. Fermin, K. Ito, C. F. van Nostrum, T. Vermonden, *Multifunct. Mater.* **2021**, 4, 032001.
- [92] X. Li, Q. Sun, Q. Li, N. Kawazoe, G. Chen, *Front. Chem.* **2018**, 6, 499.
- [93] E. Prince, J. Cruickshank, W. Ba-Alawi, K. Hodgson, J. Haight, C. Tobin, A. Wakeman, A. Avoulov, V. Topolskaia, M. J. Elliott, A. P. McGuigan, H. K. Berman, B. Haibe-Kains, D. W. Cescon, E. Kumacheva, *Nat. Commun.* **2022**, 13, 1466.
- [94] a) T. Jiang, J. Zhao, S. Yu, Z. Mao, C. Gao, Y. Zhu, C. Mao, L. Zheng, *Biomaterials* **2019**, 188, 130; b) S. Pedron, B. A. Harley, *J. Biomed. Mater. Res., Part A* **2013**, 101, 3404.
- [95] B. J. Gill, D. L. Gibbons, L. C. Roudsari, J. E. Saik, Z. H. Rizvi, J. D. Roybal, J. M. Kurie, J. L. West, *Cancer Res.* **2012**, 72, 6013.
- [96] C. Wang, X. Tong, F. Yang, *Mol. Pharm.* **2014**, 11, 2115.
- [97] D. Loessner, K. S. Stok, M. P. Lutolf, D. W. Hutmacher, J. A. Clements, S. C. Rizzi, *Biomaterials* **2010**, 31, 8494.
- [98] C. Y. Lim, J. H. Chang, W. S. Lee, K. M. Lee, Y. C. Yoon, J. Kim, I. Y. Park, *Pancreatol.* **2018**, 18, 913.
- [99] J. N. Beck, A. Singh, A. R. Rothenberg, J. H. Elisseeff, A. J. Ewald, *Biomaterials* **2013**, 34, 9486.
- [100] S. P. Singh, M. P. Schwartz, E. Y. Tokuda, Y. Luo, R. E. Rogers, M. Fujita, N. G. Ahn, K. S. Anseth, *Sci. Rep.* **2015**, 5, 17814.
- [101] W. Xiao, A. Ehsanipour, A. Sohrabi, S. K. Seidlits, *J. Visualized Exp.* **2018**, 58176.
- [102] A. V. Taubenberger, L. J. Bray, B. Haller, A. Shaposhnikov, M. Binner, U. Freudenberg, J. Guck, C. Werner, *Acta Biomater.* **2016**, 36, 73.
- [103] a) L. A. Sawicki, E. M. Ovadia, L. Pradhan, J. E. Cowart, K. E. Ross, C. H. Wu, A. M. Kloxin, *APL Bioeng.* **2019**, 3, 016101; b) C. L. Hede-gaard, C. Redondo-Gomez, B. Y. Tan, K. W. Ng, D. Loessner, A. Mata, *Sci. Adv.* **2020**, 6, eabb3298; c) Y. Iwamoto, Y. Fujita, Y. Sugioka, *Clin. Exp. Metastasis* **1992**, 10, 183.
- [104] E. Bigaeva, J. J. M. Bomers, C. Biel, H. A. M. Mutsaers, I. A. M. de Graaf, M. Boersema, P. Olinga, *Toxicol. In Vitro* **2019**, 59, 312.
- [105] D. S. Straus, *Life Sci.* **1981**, 29, 2131.
- [106] H. Modjtahedi, S. Essapen, *Anticancer Drugs* **2009**, 20, 851.
- [107] H. Xu, X. Lyu, M. Yi, W. Zhao, Y. Song, K. Wu, *J. Hematol. Oncol.* **2018**, 11, 116.
- [108] S. Misra, C. F. Moro, M. Del Chiaro, S. Pouso, A. Sebestyen, M. Lohr, M. Bjornstedt, C. S. Verbeke, *Sci. Rep.* **2019**, 9, 2133.
- [109] B. Majumder, U. Baraneedharan, S. Thiyagarajan, P. Radhakrishnan, H. Narasimhan, M. Dhandapani, N. Brijwani, D. D. Pinto, A. Prasath, B. U. Shanthappa, A. Thayakumar, R. Surendran, G. K.

- Babu, A. M. Shenoy, M. A. Kuriakose, G. Bergthold, P. Horowitz, M. Loda, R. Beroukham, S. Agarwal, S. Sengupta, M. Sundaram, P. K. Majumder, *Nat. Commun.* **2015**, *6*, 6169.
- [110] J. T. Neal, X. Li, J. Zhu, V. Giangarra, C. L. Grzeskowiak, J. Ju, I. H. Liu, S. H. Chiou, A. A. Salahudeen, A. R. Smith, B. C. Deutsch, L. Liao, A. J. Zemek, F. Zhao, K. Karlsson, L. M. Schultz, T. J. Metzner, L. D. Nadauld, Y. Y. Tseng, S. Alkhairi, C. Oh, P. Kesula, D. Mendoza-Villanueva, F. M. De La Vega, P. L. Kunz, J. C. Liao, J. T. Leppert, J. B. Sunwoo, C. Sabatti, J. S. Boehm, et al., *Cell* **2018**, *175*, 1972.
- [111] V. G. LeBlanc, D. L. Trinh, S. Aslanpour, M. Hughes, D. Livingstone, D. Jin, B. Y. Ahn, M. D. Blough, J. G. Cairncross, J. A. Chan, J. J. P. Kelly, M. A. Marra, *Cancer Cell* **2022**, *40*, 379.
- [112] D. He, D. Wang, P. Lu, N. Yang, Z. Xue, X. Zhu, P. Zhang, G. Fan, *Oncogene* **2021**, *40*, 355.
- [113] a) R. Browaeys, W. Saelens, Y. Saeys, *Nat. Methods* **2020**, *17*, 159; b) L. J. W. Tang, A. Zaseela, C. C. M. Toh, C. Adine, A. O. Aydar, N. G. Iyer, E. L. S. Fong, *Adv. Drug Delivery Rev.* **2021**, *175*, 113817; c) M. Efremova, M. Vento-Tormo, S. A. Teichmann, R. Vento-Tormo, *Nat. Protoc.* **2020**, *15*, 1484.
- [114] S. Black, D. Phillips, J. W. Hickey, J. Kennedy-Darling, V. G. Venkataaraman, N. Samusik, Y. Goltsev, C. M. Schurch, G. P. Nolan, *Nat. Protoc.* **2021**, *16*, 3802.
- [115] E. R. Parra, N. Uraoka, M. Jiang, P. Cook, D. Gibbons, M. A. Forget, C. Bernatchez, C. Haymaker, I. I. Wistuba, J. Rodriguez-Canales, *Sci. Rep.* **2017**, *7*, 13380.
- [116] a) D. R. Ahlf Wheatcraft, X. Liu, A. B. Hummon, *J. Visualized Exp.* **2014**, e52313; b) B. P. David, O. Dubrovskiy, T. E. Speltz, J. J. Wolff, J. Frasier, L. M. Sanchez, T. W. Moore, *ACS Med. Chem. Lett.* **2018**, *9*, 768.
- [117] A. L. Bulin, T. Hasan, *Methods Mol. Biol.* **2022**, *2451*, 81.
- [118] A. S. Genshaft, C. G. K. Ziegler, C. N. Tzouanas, B. E. Mead, A. M. Jaeger, A. W. Navia, R. P. King, M. D. Mana, S. Huang, V. Mitsialis, S. B. Snapper, O. H. Yilmaz, T. Jacks, J. F. Van Humbeck, A. K. Shalek, *Nat. Commun.* **2021**, *12*, 4995.
- [119] S. R. Kantelhardt, W. Caarls, A. H. de Vries, G. M. Hagen, T. M. Jovin, W. Schulz-Schaeffer, V. Rohde, A. Giese, D. J. Arndt-Jovin, *PLoS One* **2010**, *5*, e11323.
- [120] B. D. Groff, A. W. L. Kinman, J. F. Woodroof, R. R. Pompano, *J. Immunol. Methods* **2019**, *464*, 119.
- [121] L. F. Horowitz, A. D. Rodriguez, A. Au-Yeung, K. W. Bishop, L. A. Barner, G. Mishra, A. Raman, P. Delgado, J. T. C. Liu, T. S. Gujral, M. Mehrabi, M. Yang, R. H. Pierce, A. Folch, *Lab Chip* **2021**, *21*, 122.
- [122] J. Neev, F. G. Will, S. Nolte, T. Block, P. Menne, A. Heisterkamp, C. B. Schaffer, H. Lubatschowski, *Proc. SPIE* **2007**, *6460*, 646007-1.
- [123] a) R. E. Friedrich, M. Quade, N. Jowett, P. Kroetz, M. Amling, F. K. Kohlusch, J. Zustin, M. Gosau, H. Schlüter, R. J. D. Miller, *In Vivo* **2020**, *34*, 2325; b) B. S. Kowtharapu, C. Marfurt, M. Hovakimyan, F. Will, H. Richter, A. Wree, O. Stachs, R. F. Guthoff, *J. Microsc.* **2017**, *265*, 21.
- [124] H. Wang, J. D. Owens, J. H. Shih, M. C. Li, R. F. Bonner, J. F. Mushinski, *BMC Genomics* **2006**, *7*, 97.
- [125] J. C. T. Lim, J. P. S. Yeong, C. J. Lim, C. C. H. Ong, S. C. Wong, V. S. P. Chew, S. S. Ahmed, P. H. Tan, J. Iqbal, *Pathology* **2018**, *50*, 333.
- [126] C. Giesen, H. A. Wang, D. Schapiro, N. Zivanovic, A. Jacobs, B. Hatendorf, P. J. Schuffler, D. Grolimund, J. M. Buhmann, S. Brandt, Z. Varga, P. J. Wild, D. Gunther, B. Bodenmiller, *Nat. Methods* **2014**, *11*, 417.
- [127] a) W. C. C. Tan, S. N. Nerurkar, H. Y. Cai, H. H. M. Ng, D. Wu, Y. T. F. Wee, J. C. T. Lim, J. Yeong, T. K. H. Lim, *Cancer Commun.* **2020**, *40*, 135; b) M. Allam, S. Cai, A. F. Coskun, *npj Precis. Oncol.* **2020**, *4*, 11; c) H. Ahsan, R. Ahmad, *Rheumatol. Autoimmun.* **2022**, *2*, 120.
- [128] L. F. Horowitz, A. D. Rodriguez, Z. Dereli-Korkut, R. Lin, K. Castro, A. M. Mikheev, R. J. Monnat Jr., A. Folch, R. C. Rostomily, *npj Precis. Oncol.* **2020**, *4*, 12.
- [129] J. Sun, W. Liu, Y. Li, A. Gholamipour-Shirazi, A. Abdulla, X. Ding, *Microfluid. Nanofluid.* **2017**, *21*, 1.
- [130] F. Eduati, R. Utharala, D. Madhavan, U. P. Neumann, T. Longrich, T. Cramer, J. Saez-Rodriguez, C. A. Merten, *Nat. Commun.* **2018**, *9*, 2434.
- [131] J. Sun, A. R. Warden, X. Ding, *Biomicrofluidics* **2019**, *13*, 061503.
- [132] F. Xing, Y. C. Liu, S. Huang, X. Lyu, S. M. Su, U. I. Chan, P. C. Wu, Y. Yan, N. Ai, J. Li, M. Zhao, B. K. Rajendran, J. Liu, F. Shao, H. Sun, T. K. Choi, W. Zhu, G. Luo, S. Liu, L. Xu, K. L. Chan, Q. Zhao, K. Miao, K. Q. Luo, W. Ge, X. Xu, G. Wang, T. M. Liu, C. X. Deng, *Theranostics* **2021**, *11*, 9415.
- [133] a) J. Sumbal, A. Chiche, E. Charifou, Z. Koledova, H. Li, *Front. Cell Dev. Biol.* **2020**, *8*, 68; b) B. Bian, N. A. Juiz, O. Gayet, M. Bigonnet, N. Brandone, J. Roques, J. Cros, N. Wang, N. Dusetti, J. Iovanna, *Front. Oncol.* **2019**, *9*, 475.
- [134] X. Gong, Z. Liang, Y. Yang, H. Liu, J. Ji, Y. Fan, *Regener. Biomater.* **2020**, *7*, 271.
- [135] K. Kenefick, Real-Time Analysis for Cell Viability, Cytotoxicity and Apoptosis: What Would You Do with More Data from One Sample? **2022**, <https://www.promegaconnections.com/real-time-analysis-for-cell-viability-cytotoxicity-and-apoptosis-what-would-you-do-with-more-data-from-one-sample/>.
- [136] J. Whiteford, S. Arokiasamy, C. L. Thompson, N. P. Dufton, *In Vitro Models* **2022**, *1*, 413.
- [137] a) S. Y. Lee, M. K. Ju, H. M. Jeon, E. K. Jeong, Y. J. Lee, C. H. Kim, H. G. Park, S. I. Han, H. S. Kang, *Oxid. Med. Cell. Longevity* **2018**, *2018*, 3537471; b) J. A. Nagy, S. H. Chang, A. M. Dvorak, H. F. Dvorak, *Br. J. Cancer* **2009**, *100*, 865.
- [138] A. J. Najibi, D. J. Mooney, *Adv. Drug Delivery Rev.* **2020**, *161*, 42.
- [139] T. Fischetti, G. Di Pompo, N. Baldini, S. Avnet, G. Graziani, *Cancers* **2021**, *13*, 4065.
- [140] E. P. Chen, Z. Toksoy, B. A. Davis, J. P. Geibel, *Front. Bioeng. Biotechnol.* **2021**, *9*, 664188.
- [141] L. Neufeld, E. Yeini, N. Reisman, Y. Shtilerman, D. Ben-Shushan, S. Pozzi, A. Madi, G. Tiram, A. Eldar-Boock, S. Ferber, R. Grossman, Z. Ram, R. Satchi-Fainaro, *Sci. Adv.* **2021**, *7*, eabi9119.
- [142] Y. Nashimoto, R. Okada, S. Hanada, Y. Arima, K. Nishiyama, T. Miura, R. Yokokawa, *Biomaterials* **2020**, *229*, 119547.
- [143] a) Z. Hu, Y. Cao, E. A. Galan, L. Hao, H. Zhao, J. Tang, G. Sang, H. Wang, B. Xu, S. Ma, *ACS Biomater. Sci. Eng.* **2022**, *8*, 1215; b) J. Lim, H. Ching, J. K. Yoon, N. L. Jeon, Y. Kim, *Nano Convergence* **2021**, *8*, 12.
- [144] K. Haase, G. S. Offeddu, M. R. Gillrie, R. D. Kamm, *Adv. Funct. Mater.* **2020**, *30*, 2002444.
- [145] a) A. Boussommier-Calleja, Y. Atiyas, K. Haase, M. Headley, C. Lewis, R. D. Kamm, *Biomaterials* **2019**, *198*, 180; b) J. Song, H. Choi, S. K. Koh, D. Park, J. Yu, H. Kang, Y. Kim, D. Cho, N. L. Jeon, *Front. Immunol.* **2021**, *12*, 733317.
- [146] K. M. van Pul, M. F. Fransen, R. van de Ven, T. D. de Gruijl, *Front. Immunol.* **2021**, *12*, 643291.
- [147] S. Shim, M. C. Belanger, A. R. Harris, J. M. Munson, R. R. Pompano, *Lab Chip* **2019**, *19*, 1013.
- [148] a) Y. C. S. Ramon, M. Sese, C. Capdevila, T. Aasen, L. De Mattos-Arruda, S. J. Diaz-Cano, J. Hernandez-Losa, J. Castellvi, *J. Mol. Med.* **2020**, *98*, 161; b) A. Marusyk, M. Janiszewska, K. Polyak, *Cancer Cell* **2020**, *37*, 471; c) J. Liu, H. Dang, X. W. Wang, *Exp. Mol. Med.* **2018**, *50*, e416.
- [149] a) L. Businaro, A. De Nino, G. Schiavoni, V. Lucarini, G. Ciasca, A. Gerardino, F. Belardelli, L. Gabriele, F. Mattei, *Lab Chip* **2013**, *13*, 229; b) S. Parlato, A. De Nino, R. Molfetta, E. Toschi, D. Salerno, A. Mencattini, G. Romagnoli, A. Fragale, L. Roccazzello, M. Buoncervello, I. Canini, E. Bentivegna, M. Falchi, F. R. Bertani, A. Ger-

- ardino, E. Martinelli, C. Natale, R. Paolini, L. Businaro, L. Gabriele, *Sci. Rep.* **2017**, 7, 1093.
- [150] Z. Ao, H. Cai, Z. Wu, L. Hu, A. Nunez, Z. Zhou, H. Liu, M. Bondeson, X. Lu, X. Lu, M. Dao, F. Guo, *Proc. Natl. Acad. Sci. U. S. A.* **2022**, 119, e2214569119.
- [151] a) A. T. L. Truong, L. W. J. Tan, K. A. Chew, S. Villaraza, P. Siongco, A. Blasiak, C. Chen, D. Ho, *Adv. Ther.* **2021**, 4, 2100091; b) M. Rashid, T. B. Toh, L. Hooi, A. Silva, Y. Zhang, P. F. Tan, A. L. Teh, N. Karnani, S. Jha, C. M. Ho, W. J. Chng, D. Ho, E. K. Chow, *Sci. Transl. Med.* **2018**, 10, eaan0941.



Kenny Zhuoran Wu received his B.S. degree and his M.Eng. degree from the South China University of Technology and Nanyang Technological University, respectively. He was admitted to the National University of Singapore in 2022 and is currently in his first year of doctoral program at the Translational Tumor Engineering (TTE) Laboratory in the Department of Biomedical Engineering. His current research is focused on engineering stromal heterogeneity using in vitro tumor niches and developing clinically applicable tumor models for high-throughput cancer drug testing.



Christabella Adine is a research fellow with TTE Laboratory at the National University of Singapore (NUS). She has a strong interest in tissue engineering, cancer model development, and personalized medicine. Specifically, she is working on developing personalized tumor models using biomaterial engineering for head and neck cancer patients with the goal of improving patient outcomes through more accurate and effective treatment plans. This research has the potential to revolutionize how cancer is treated. Her Ph.D. from NUS in tissue engineering and regenerative medicine provided her with a solid foundation in these areas.



Aleksandr Mitriashkin is a Ph.D. student at the Translational Tumor Engineering Laboratory, Department of Biomedical Engineering, National University of Singapore. Starting from the field of 3D bioprinting, Aleksandr gets enthusiastic for 3D spheroids and scaffoldless tissue engineering methods. Now his main interests are in recapitulation of tumor–stroma interactions in 3D cell models and in tuning cells' state by micropatterning to recreate different tumor stroma traits. He believes that research cancer in 3D as well as on a single cell level could shed light on its malignancy and resistivity.



Eliza Fong is an assistant professor in the Department of Biomedical Engineering at the National University of Singapore. Most cancer patients do not receive individualized drug treatment regimes. Rather, they receive “standard-of-care” regimens where they are treated with drugs that are known to “work” for a general cohort of patients with the same cancer type. Leading the Translational Tumor Engineering (TTE) Laboratory, Dr. Fong and her team leverage biomaterials engineering strategies and other bioengineering tools to develop platforms to either reconstruct or maintain patient tumor tissues outside the body for personalized drug testing.